DETECTING INCISED VALLEY-FILL SANDSTONE IN BEAUCHAMP FIELD BY USING SEISMIC ATTRIBUTES, STANTON COUNTY, USA

by

SAAD ABDULLAH ALMALKI

B.S., King Saud University, 2009

A THESIS

Submitted in partial fulfillment of the requirements for the degree

MASTER OF SCIENCE

Department of Geology
College of Arts and Sciences

KANSAS STATE UNIVERSITY
Manhattan, Kansas

2013

Approved by:

Major Professor

Matthew W Totten

Abstract

A 3D seismic survey was conducted on Beauchamp, Beauchamp North and Beauchamp Northwest fields, which are located in Stanton County, southwest Kansas, by Berexco, Inc. Stanton County is situated on the Hugoton embayment which is the shelf of the Anadarko basin. The producing formation in this area is the Morrow formation, which is the lower Pennsylvanian period. The Morrow formation is mostly a clastic unit and its base was transgressive marine. It is considered an unconformity lying on the Mississippian rocks. Wide geologists agreed with the name of Morrow as name in the rock stratigraphic sequence in the study area (Forgotson, et al., 1966). "The Morrowan series is defined as the interval between the base of the Atokan Thirteen finger limestones and the top of the pre-Pennsylvanian unconformity" (Puckette, et al., 1996). The depositional environment of upper Morrow Formation in western Kansas, according to Sonnenberg (1985), Krystinik et al (1990), was a valley-fill deposit. The purpose of this study is to focus on detecting valley-fill sandstone in the study area by using appropriate seismic attributes. Coherence and discontinuity along dip succeeded to map incised valley-fill sandstone width. On another hand, spectral decomposition displayed subtle changes in incised valley thickness. Positive curvature shows valley edges in moderate resolution, but the most negative curvature wasn't clear enough to display the valley-fill sand. The result of RMS amplitude and average energy attributes results were almost the same. They exhibited four areas of high amplitude and energy in the valley which may indicate the presence of hydrocarbon. Sweetness and envelope amplitude both detected the valley in the study area. A gamma ray cross section shows that there are sequences of incised valley-fill sandstone which are sandstone A, B, C and D of the upper Morrow formation. Johns 2-12 well is producing oil from lower Morrow and sandstone A, thus the valley in the study area may produce oil from Sandstone A or B as RMS amplitude and average anergy showing high amplitude in four areas in the valley.

Table of contents

List of Figures

List of Tables

Acknowledgements

I would like to thank Dr Matthew Totten for his help and his cooperation with me and accepting me as graduate student. I would like also to thank Dr Sambhudas Chaudhuri and Dr. Matthew Brueseke for their help and their cooperation.

I also strongly thank Kuwait United Company (KUS) for helping me and allowing me to work on their facility and with their experts in geophysics field. Special thanks to Mohammed Alresheed, Mohammed Omran, Prashant Bansal and Sarper for their help and instructions.

I also would like to thank King Abdulaziz City for Science and Technology(KACST) for sponsoring my studies at KSU.

Dedication

I would like to dedicate this thesis to my father and my mother and my wife for their encouragements and supports.

Chapter 1 – Introduction

Study Area:

The study area is located in Stanton County which is in the southwestern corner of Kansas. A 3D Seismic survey was collected by BEREXCO LLC in 2007 to develop the producing oil and gas reservoirs. This survey covers three fields; the Beauchamp, Beauchamp North, and Beauchamp Northwest Fields. Figure 1-2 shows the location of these fields and the 3D Seismic survey. The Beauchamp North field has produced around 516,345 barrels of oil and around 722,992 Mcf of gas since discovered in 1984. The Beauchamp field has produced around 1,241,142 barrels of oil since 1966, and it has produced around 16,365,808 Mcf of gas since it was discovered in 1968. The Beauchamp Northwest field produced around 20,117 barrels of oil between 1983 and 1991.

The major producing formation at these fields is the Morrow formation. The Morrow formation is in the Lower part of the Pennsylvanian system. This formation was formed in the Hugoton Embayment of the Anadarko basin. These are considered as stratigraphic traps.

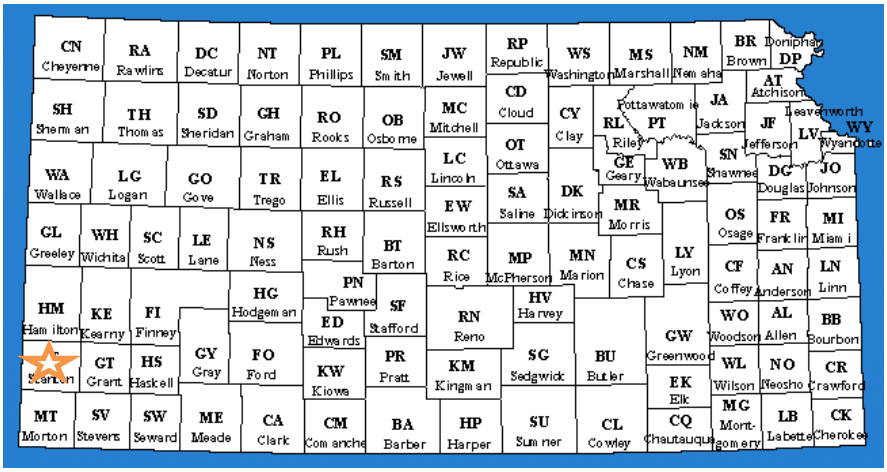

Figure 1-1 Counties of Kansas and the postion of Stanton County.

---

[2] **Modified from (**Kansas academy science)

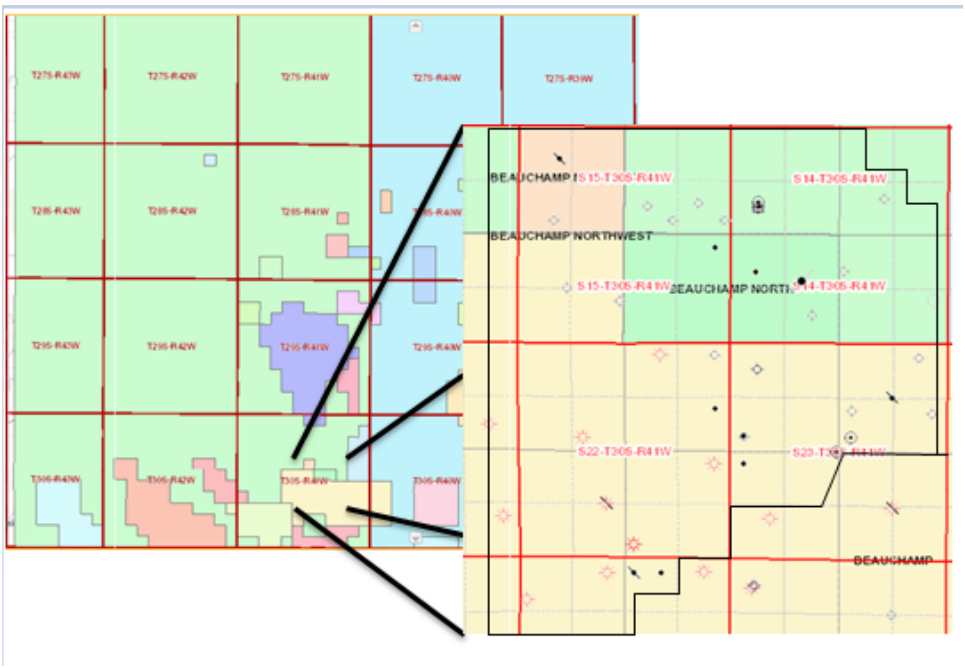

Figure 1-2 Maps illustrating Stanton County, the position of study area and seismic survey boundary, which includes Beauchamp field, Beauchamp North field and Beauchamp Northwest field[3]

---

[3] **Modified from (Kansas Geological Survey)**

Chapter 2 - Geological Background

Paleogeography of Morrow formation:

During the Pennsylvanian Period, there were many tectonic events on the south-central of North America (Moore, 1979). These tectonic events caused the rising of sea level towards the land (marine transgression). In addition, the changing paleoclimate caused erosion; transporting new material for deposition in the basin (Schopf, 1975).

The variation in sediments from one region to another and the pattern of deposition within the south-central region of North America during the Pennsylvanian period took place because of many events that happened at that time. Figure 2-1 shows the location of Stanton County close to equator during the Mississippian and Pennsylvanian periods and the position of relevant structural features (Sonnenberg et al., 1990). Pennsylvanian period events are summarized in the following: first, the Ouachita Mountains, Amarillo-Wichita uplift, Ancestral

Rockies-Apishapa uplift, and other uplifts of more local influence were provided sediments sources; second, destruction of Ouachita seaway; third, creating basin of Anadarko; fourth, flooding in north of south-central of North America and cratonic sources that came from northeast became less important (Moore, 1979).

"The Pennsylvanian flora of the coal measures in the Appalachian region is an impressive record of plant growth in a warm, humid climate. Evidence that the climate indicated by the Pennsylvanian coal flora was in fact tropical or subtropical was presented by White (1913, 1932) and Potonie (1911). Areas within the Appalachian coal field and the northern European coal fields represent the warmest and most humid climates of which a record is available. If North America and Europe lay adjacent during Pennsylvanian time, a line drawn lengthwise through these coal fields might indicate the axis of a tropical zone now displaced northward. The equator shown on the map corresponds to the present site of the Appalachian coal field, suggesting that most of the United States may have been within the tropical or subtropical zone north of the equator during Pennsylvanian time. The maximum distance from the equator would have been about 2,000 miles or roughly the distance that southern Florida or Texas now is north of the equator" (Schopf, 1975). Figure 2-2 shows the paleogeography of Kansas during the late of Mississippian and the early of Pennsylvanian periods. A lot of the south-central region of North America area was situated near the equator. Broad shallow cratonic seas covered much of the Mid-Continent area (Sonnenberg et al., 1990).

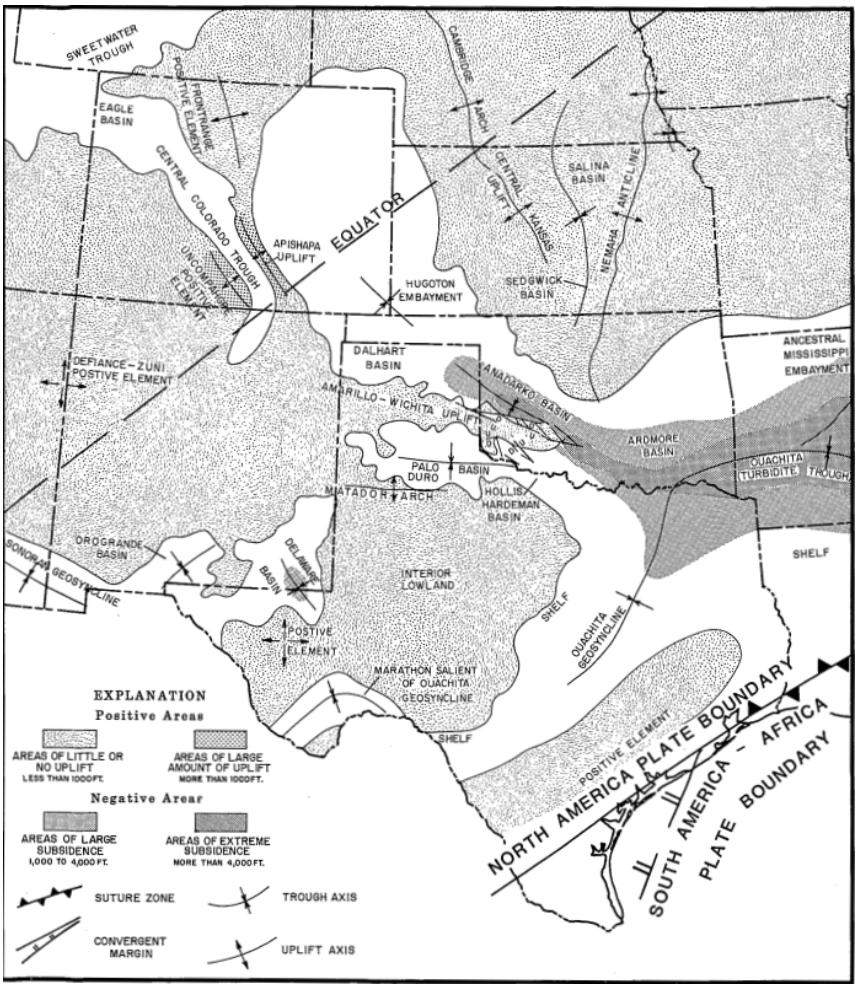

Figure 2-1 Map showing the location of Stanton County close to equator during Mississippian and Pennsylvanian periods and structural features [4].

---

[4] Modified from (Sonnenberg et al., 1990)

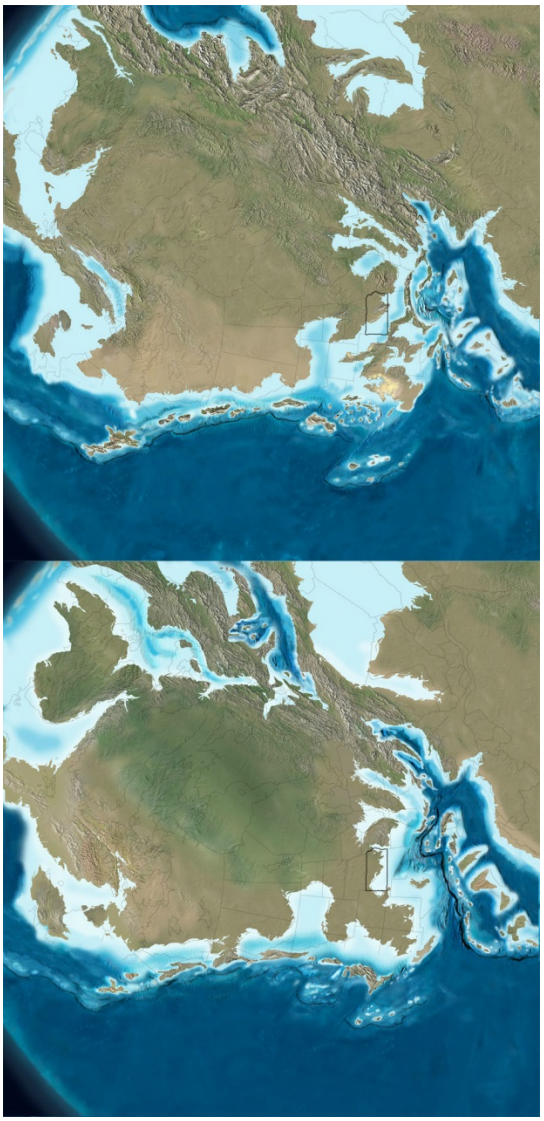

Figure 2-2 Two maps showing the position of Kansas during Late Mississippian 325 Ma (Left) and Early Pennsylvanian 315 Ma[5]

---

[5] Modified from (Northern Arizona University, Paleogeography and Geologic Evolution of North America)

Structure:

Stanton County is situated on the Hugoton embayment along the shelf of the Anadarko basin. The Wichita-Amarillo uplift borders the basin on the south and the Cimarron arch on the west. The central Kansas uplift and the Las Animas arch border the Anadarko basin on the north,

and the Nemaha ridge on the east. The very asymmetrical nature of the Anadarko basin was caused by rapid subsidence in the southern part of the basin, and creating faults due to the Pennsylvanian orogeny (Puckette et al., 1996). Figure 2-1 illustrates the structural features during Morrowan period.

Structural lineaments in many areas were caused by two tectonic events, a pre-Morrowan to Late Mississippian cratonic epeirogeny, and the early Middle Pennsylvanian Wichita Orogeny (Rascoe and Adler, 1983; Sonnenberg et al., 1990).

A Lower Pennsylvanian unconformity exists along the base of the Morrowan. This Lower Pennsylvanian unconformity covered much of the south-central region of North America during pre-Morrowan period while erosion happened at this time. The Cambridge Arch and Central Kansas Uplift were created during this period (Rascoe and Adler, 1983;Sonnenberg et al., 1990).

The rapid subsidence affected the Anadarko basin more than in the shelf of Anadarko basin which is located in western Kansas and southeastern of Colorado. The upper Mississippian didn't exhibit much erosion at the deep areas of the Anadarko basin and some area may have continuity in sedimentation to the early of Pennsylvanian period (Sonnenberg et al., 1990).

Stratigraphy:

The Morrow formation is mostly a clastic unit, and its base is transgressive marine. It lies unconformably on the Mississippian rocks. Most geologists agreed with the name of Morrow as name in the stratigraphic sequence in the study area (Forgotson, et al., 1966). "The Morrowan series is defined as the interval between the base of the Atokan "Thirteen finger limestone" and the top of the pre-Pennsylvanian unconformity" (Puckette et al., 1996),

There are three subdivisions of the Morrow formation in the Hugoton embayment. First, the Morrow formation can be divided into four units which are Keyes limestone, lower marine shale, middle sandstone and upper marine shale (Sonnenberg et al., 1990). Second, it is three units which are sandy lower unit, limestone and shale sequences middle unit and shaly upper unit (Forgotson et al., 1966). Third, it is divided into two units, upper and lower Morrow and squaw belly limestone is used to separate between them (Al-Shaieb et al., 1995). Figure 2-3 shows the stratigraphic distribution of oil and gas production in Kansas. This figure shows Morrow formation lying on Chesteran stage and underlying by Atokan stage and shows that morrow formation produces oil and gas in Kansas. Red dash highlighted Morrow formation.

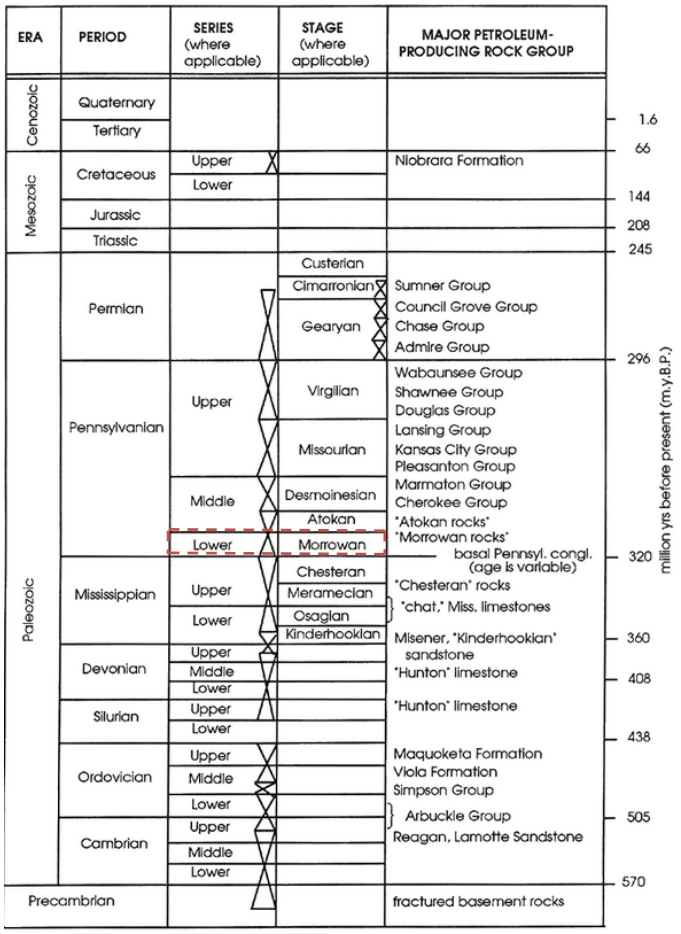

Figure3 -3 The stratigraphy column of Kansas and geologic timetable showing distribution of oil and gas production in Kansas[6]

Modified from (Stratigraphic and Spatial Distribution of Oil and Gas Production in Kansas by Newell et al.,)

Depositional Environment:

Mississippian topography was exposed to erosion and detritus was deposited to form marine sandstones in the lower Morrow formation. According to (Wheeler et al., 1990), the depositional facies was a shoreface, while Gerken,(1992) said that depositional facies was transgressive valley-fill sandstones. On the upper Morrow formation, the predominant sediments were fluvial sand and marine muds (Al-Shaieb et al., 1995).The depositional environment of upper Morrow formation in western Kansas, according to Swanson() was a coastal-plain fluvial to delta. Recently, the depositional environment of upper Morrow formation in western Kansas, according to Sonnenberg (1985), and Krystinik et al, (1990), has been interpreted as valley-fill deposits.

The Anadarko basin was extended from Oklahoma into southwestern Kansas and southeastern Colorado because of rapid subsidence in the deep Anadarko basin, which shallows depth towards Kansas and Colorado. The southern part of the Anadarko basin was home to prograding alluvial fan and fan deltas, because the sediments shed from shallow shelf to deep basin. In contrast, on the northern, more gentle flank of the Anadarko Basin, shelf-margin deltaic deposits were fed by a broad drainage network which covered much of eastern Colorado and western Kansas. Glacio-eustasy occurred at early Pennsylvanian time resulting in a shift of shoreline. "During glacially-induced sea-level lowstands, eastern Colorado and western Kansas were subject to subaerial exposure and the establishment of drainage patterns and valley incision" (Kristinik and Blakeny,1990). Because of rising and decreasing a shoreline in southwestern Kansas and southeastern Colorado (figure 2-4), transgression and regression marine created a lot of valley-fill in Morrow formation. "Morrow valley-fills are typically blocky to fining upward sandstone deposits but can be heterolithic assemblages of sandstone and mudstone" (Kristinik, L and B. Blakeny, 1990).

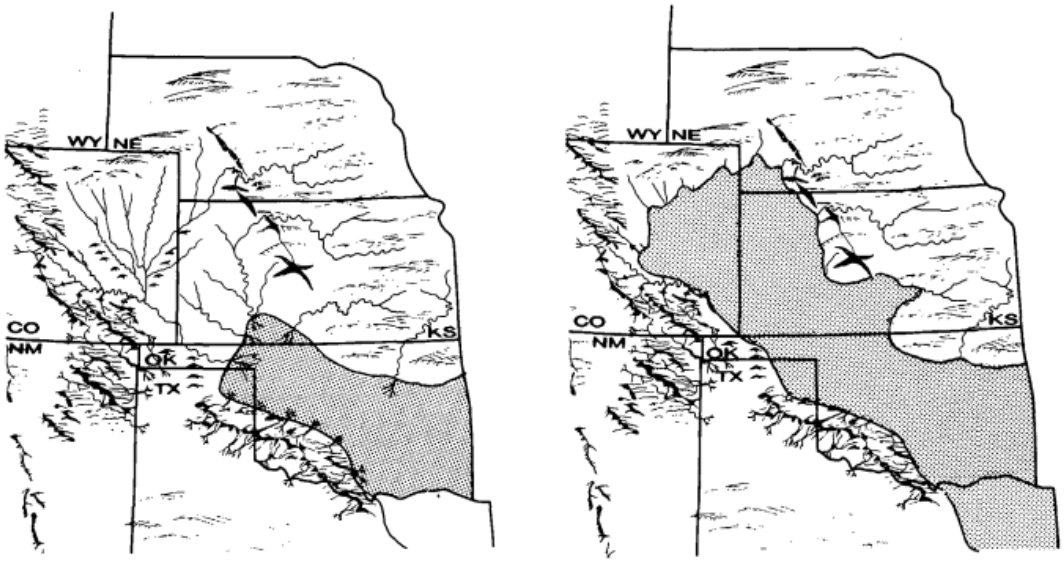

Figure 2-4 Two maps showing the transgression marine (highstands) and regression marine (lowstands)[7]..

---

[7] **Modified from (Roscoe, 1978, Swanson, 1979 and Sonnenberg, 1985).**

Chapter 3 - Methodology

The primary software used in this study is Petrel by Schlumberger and Seiswork by Halliburton. A brief summary of software features used in this study follows below. The available data in study area is migrated 3D seismic, and well logs which include Gamma ray, sonic, and density, within the survey boundary.

The 3D seismic survey was conducted in Beauchamp North, Beauchamp Northwest and Beauchamp fields in 2007 by BEREXCO INC. The seismic data from field was processed by Sterling Seismic Services, Ltd in December 2007. This survey covered approximately 3.5 square miles, which has 144 inlines and 132 crosslines. Inlines ran from west to east and Xlines ran from south to north. The datum of this survey was 3500 feet, and the velocity replacement was 10000 F/S. The dataset file was SEG-Y standard format and the sampling rate was 2 millisecond. The projection system of the survey was NAD27, Kansas-South in feet. The 3D seismic dataset was the first data from the study area.

Other available data included well logs on three wells that have sonic log and density log in LAS format. Others wells, which are located on the seismic survey boundary, are in TIFF format. A few wells do not have logs. Wells that were used in this study are Dickey-Robb 1, Gwinner 'Z' 2 and Beauchamp 'B' 1. Other useful information from these wells include formation tops, total depth, elevation, Kelly bushing elevation (KB), status of production and coordinates of their locations. The three digital LAS sonic logs and density logs of the three wells downloaded from the Kansas Geological Survey website were converted from TIFF format to LAS format using NeuraLog software. Several other wells were also downloaded, which aren't located on the seismic survey boundary, from the Kansas Geological Survey website in TIFF format to make gamma ray cross sections of Beauchamp 'B' 1 with, Love 5, Barnhardt 1, Barnhardt 3, Johns 2-12 and Johns 3-12. Table 3-1 illustrates the wells that are located on the study area and their information. Table 3-2 illustrates the wells used for tying synthetic seismograms to seismic data. Table 3-3 shows the wells that are located near the survey boundary and their information such as elevation, depth and formations tops.

LEASE	**WELL**	**ELEVATION (ft)**	**ELEV_REF**	**DEPTH (ft)**	**STATUS**	**formation Tops**
NAOMI	4-SWD	3367	GL	5549	SWD	yes
Naomi	2	3372	KB	5675	OIL	yes
NAOMI	3	3371	KB	5600	D&A	yes
Barnhardt 'A'	1	3364	KB	5550	D&A	no
Milburn	1	3364	KB	5549	D&A	yes
Naomi	4	3367	GL	5549	OTHER(WATER)	no
NAOMI OWWO	4-SW	3368	TOPO	1680	OTHER()	no
Naomi	1	3378	KB	5550	OIL	yes
Bosley	14-Jan	3363	KB	5380	D&A	yes
NAOMI UNIT	2-X	3361	TOPO	5675	EOR	no
Naomi	4	3360	GL		LOC	no
GWINNER 'Z'	2	3382	KB	5610	D&A	yes
ELIZABETH	2	3382	GL	5570	D&A	yes
Dickey	1	3395	KB	5585	D&A	yes
ZIMMERMAN	1	3407	KB	5507	D&A	yes
MILDRED	1	3394	KB	5670	D&A	yes
ELIZABETH	1	3395	KB	5750	OIL-P&A	yes
Dickey-Robb	1	3381	KB	5601	OIL	yes
GWINNER 'Z'	1	3395	KB	5615	D&A	yes

Zimmerman Unit 'T'	1	3375	KB	5575	D&A	yes
CARRIE 'C'	2	3386	KB	5560	GAS	no
Hilty	22-Feb	3394	KB	5625	GAS	no
CARRIE 'B'	1	3379	KB	5550	D&A	yes
CARRIE 'C'	1	3388	KB	5700	GAS	yes
HILTY	22-Jan	3390	KB	5660	GAS-P&A	yes
CARRIE 'A'	1	3380	KB	5600	OIL	yes
Carrie 'C'	2	3386	KB	5560	GAS	yes
CARRIE	1	3380	KB	5600	GAS	yes
BEAUCHAMP 'B'	3	3364	KB	5600	D&A	yes
J. N. BEAUCHAMP	1	3357	KB	5556	OIL-P&A	yes
BEAUCHAMP	2	3369	KB	5440	OIL	yes
Beauchamp	2	3377	KB	5575	D&A	yes
BEAUCHAMP 'B'	1	3359	KB	5600	D&A	yes
JOHNS	2	3373	KB	5410	GAS	yes
MYERS	1	3371	KB	5536	GAS-P&A	yes
JOHNS	1	3369	KB	5550	OIL	yes
BEAUCHAMP	3	3363	KB	5616	D&A	yes
BEAUCHAMP	4	3355	TOPO		OTHER()	no
C. PARKS	1	3358	TOPO		OTHER()	no
Love 'A'	1	3359	KB	5560	D&A	no
BEAUCHAMP	23-Jan	3377	KB	5575	D&A	yes
Williams	1	3371	KB	5455	D&A	yes
Williams	2	3378	KB	5475	OIL	yes
JACQUART	1-27	3384	KB	5500	GAS	yes
G&G	4	3397	KB	5600	GAS	no

Table 3-1 Wells that are located on the study area and their information

Well Name	Gamma ray Log (GR)	Spontaneous Potential Log (SP)	Resistivity Log	Conductivity Log	Sonic Log (TD)	Density Log
Beauchamp B' 1	Yes	Yes	Yes	Yes	Yes	Yes
Dicky-robb 1	Yes	Yes	Yes	Yes	Yes	Yes
Gwinner 'Z' 2	Yes	Yes	Yes	Yes	Yes	Yes

Table 3-2 Wells used to create synthetic seismograms to tie seismic data

Lease	well	Elevation (ft)	Elev_ref	Depth (ft)	Status	Formation tops
Johnn	2 - 12	3355	KB	5600	Oil	Yes
Johns	3 - 12	3357	KB	5480	Oil	Yes
Barnhardt	1	3356	KB	5487	Oil	No
Barnhardt	3	3344	GL	5500	Oil	No
Love	5	3355	KB	5500	Dry well	No

Table 3-3 Wells that are located near to the survey boundary and their information

Software Features:

A brief summary of featured software used in the workflow of this study are outlined below.

1- Neuralog software:

Neuralog is software for digitizing log images from scanned well-logs (such as TIFF format) to LAS files (NeuraLog, 2013). The main features of Neuralog are the automated curve picking and the quality of output, and the ability to scan well-logs from scanner to computer immediately. For this study, three density logs were digitized from TIFF format to LAS format using Neuralog. Figures 3-1 to 3-4, display the workflows of digitizing a density log.

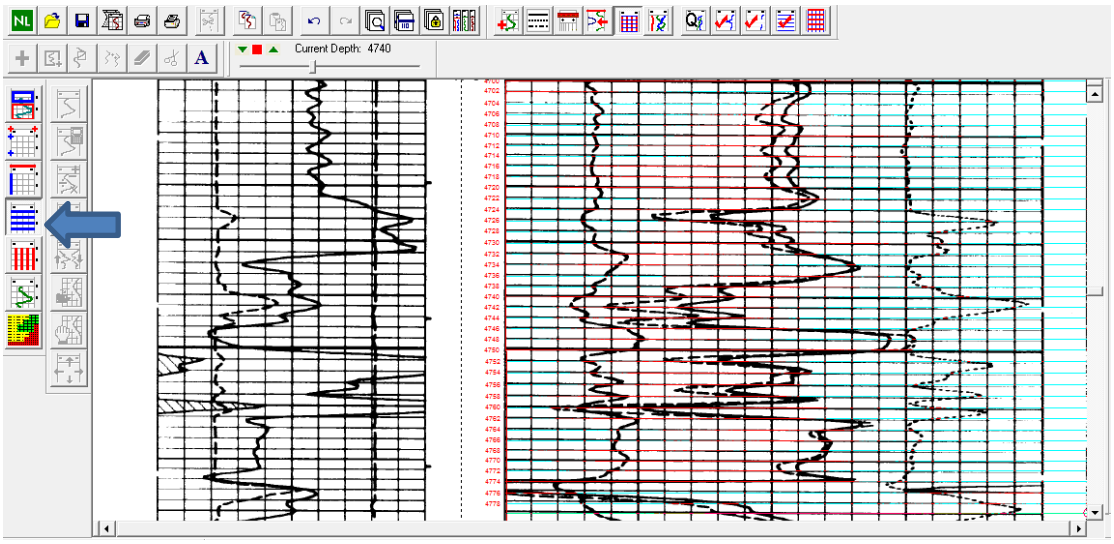

Figure 3-1 Window showing log image (density log of Gwinner Z2) from scanned log and depth grids (blue arrow).

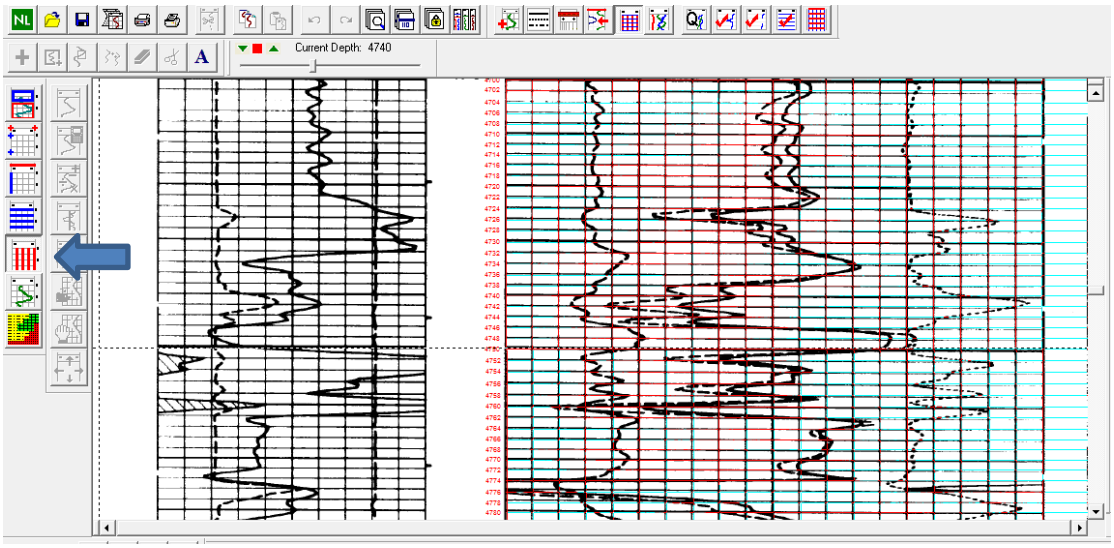

Figure 3-2 Window showing scale grids from the icon (blue arrow).

.

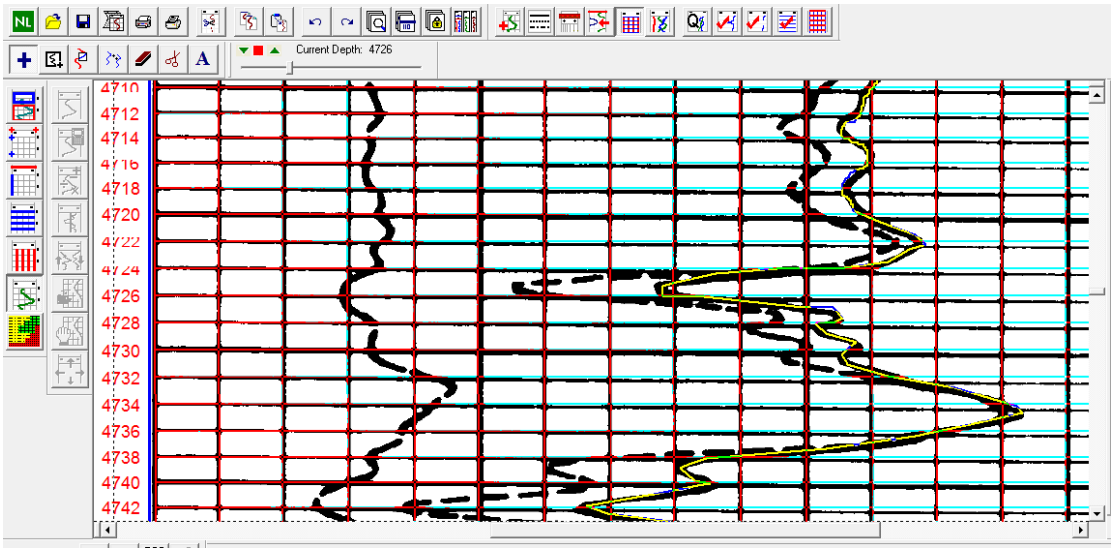

Figure 3-3 Window illustrating how to digitize density curve from well-log scanned paper (yellow color).

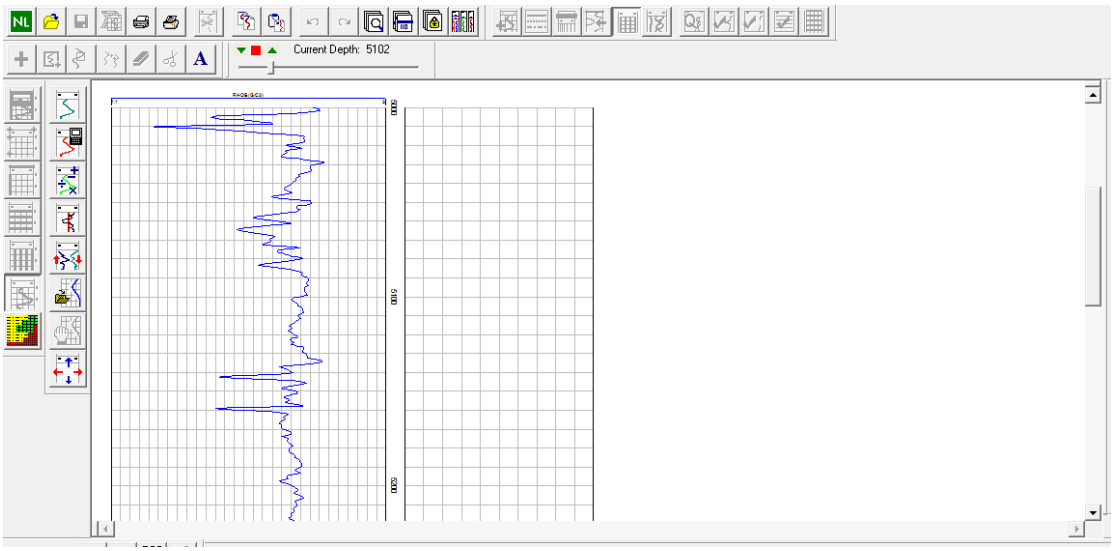

Figure 3-4 Density log in LAS format after digitizing curve in TIFF format.

2- Petrel Schlumberger:

Petrel is software that was created by Schlumberger Company for seismic interpretation and forward modeling into reservoir simulations. The 3D seismic dataset of this study area was loaded on Petrel software and average energy and envelope amplitude attributes were created using Petrel.

3- Seiswork Halliburton:

Seiswork is software that was created by Halliburton Company. The 3D seismic dataset of the study area was loaded on Seiswork, and synthetic seismogram, horizon tracking and seismic attributes were created by using Seiswork.

Synthetic Seismograms:

After loading the 3D seismic dataset and creating a base map in software and locating positions of wells on the base map, synthetic seismograms were created, which tie well log data with real seismic data. Creating a synthetic seismogram is a very important step in this process

because well log data is in the depth domain, while the 3D seismic data is in time domain. The benefit from this step is to match the formation tops, which are measured in depth in well logs, with real seismic data. Synthetic seismograms were created by multiplying the sonic log with the density log in order to calculate reflectivity, and multiplying reflectivity with a wavelet, which is obtained from real seismic data, to generate synthetic seismograms. After creating synthetic seismograms, synthetic wavelets are matched to seismic wavelets, so a time-depth conversion can be made. The horizons picked are then the closest seismic events to the formation tops.

A more narrow definition used by seismic interpreters is that a synthetic seismogram, commonly called a synthetic, is a direct one-dimensional model of acoustic energy traveling through the layers of the Earth (Schlumberger glossary oil field website).

Synthetic seismograms are generated by multiple processes. The first step multiples the velocity of layer one with the density of layer one to create the acoustic impedance of layer one, and multiples the velocity of layer two with the density of layer two to create the acoustic impedance of layer two. The second step subtracts the acoustic impedance of layer two from the acoustic impedance of layer one, and divides it by the total of adding the acoustic impedance of layer two to the acoustic impedance of layer one to create the reflection coefficient of well log data (Formula 1).

$$E(t) = (Z_2 - Z_1) / (Z_2 + Z_1) \qquad (1)$$

Where

E(t) is reflection coefficient

Z_1 is acoustic impedance ($V_1 * P_1$)

Z_2 is acoustic impedance ($V_2 * P_2$)

The third step extracts a wavelet from the real seismic data. The final step convolves the reflection coefficient of well log data with wavelet from real seismic data to generate the synthetic seismogram (Formula 2).

$$X(t) = w(t) * e(t) \qquad (2)$$

Where:

X(t) is synthetic seismogram

W(t) is seismic wavelet

E(t) is reflection coefficient

This * is meaning convolution

It is difficult to achieve 100% matching between the synthetic seismograms and real seismic data because matching depends on the quality of seismic data, which still has random noise such as multiples and other noise effects, and the quality of the well logs data. Therefore, matching between synthetic seismogram and real seismic data requires focusing on the major reflectors which guide to achieve accurate match. Synthetic seismograms sometimes need to be stretched and squeezed to be fit with real seismic data. The accurate matching between real seismic data and well log data means the accurate results in next steps in seismic interpretation because all steps after synthetic such as seismic attribute and horizon tracking depends on the accurate matching.

Horizon tracking and Surface Generation:

Horizon tracking is the second step in this study after matching synthetic seismograms with the seismic data. The purpose of doing horizon tracking is to map the formation top of interest across the seismic volume. The following steps are an explanation of the process of horizon tracking on the seismic volume. First, the synthetic seismogram of each well is displayed on the seismic section. Second, the depth to formations tops of interest are input, (upper and lower Morrow, and Chesteran), so that these tops appear on the synthetic seismogram as a small line in the seismic section. Third, the position of this line is noted on the seismic relative to the seismic wavelet. If the formation top falls on the peak amplitude, then the same peak is tracked until the end of seismic section, which is displayed in a 2D window. Likewise, if the formation top falls on a trough, then the same trough is followed. Fourth, tracking the formation top of

interest must be continued for the entire seismic volume. Finally, the same process is followed with other formation tops.

Seismic attributes:

The study of seismic attributes is an integral component of seismic interpretation. "A good seismic attribute is either directly sensitive to the desired geologic feature or reservoir property of interest, or allows us to define the structural or depositional environment and thereby enables us to infer some features or properties of interest" (Chopra and Marfurt, 2007). A seismic attribute is a measurement which is derived from seismic data, such as amplitude, phase and frequency (Schlumberger Oilfield Glossary, 2013). In this study, seismic attributes, including coherence, spectral decomposition, most positive curvature, most negative curvature , sweetness, discontinuity along dip, average energy, relative amplitude change in X and Y, RMS amplitude, and envelop amplitude were used to detect and define valley-fill sand within the study area.

Table 3-4 is a summary of the descriptions and the benefits of seismic attributes used in this study.

Seismic attribute	Description	Benefits
coherence	Coherence is seismic attribute that measures trace to trace in terms of differences and similarity in waveform.	Coherency is appropriate attribute to detect faults, fractures and channels.
discontinuity along dip	Discontinuity along dip has the same measurement of coherency but it shows faults and fracture in sharp dip cleaner than	Discontinuity along dip has the same coherency features. It reveals any discontinuity in trace amplitude like faults,

	Coherency (Halliburton website)	fractures and channels (Halliburton website).
most positive curvature	Most Positive Curvature is measure of the more positive rate of variation in reflection dip and azimuth. It focuses on display the reflection bumps.	Most positive curvature can show the channel edges very clear.
most negative curvature	Most Negative Curvature is measure of the more negative rate of variation in reflection dip and azimuth. It focuses on display the reflection drops (Halliburton-Landmark, 2011).	Most negative curvature can show channel axes (Halliburton-Landmark, 2011).
relative amplitude change in X or Y	"Relative amplitude change is the rate of change of the logarithm of the reflection strength. Computed along the x axis, relative amplitude change g_x is	"It serves as a directional high-resolution discontinuity attribute, revealing details in faults and channels viewed along time or depth slices" (Halliburton-Landmark,

	given by $g_x = \frac{\partial}{\partial x} \ln a$ where a is reflection strength. Computed along the y axis, relative amplitude change g_y is given by $g_y = \frac{\partial}{\partial y} \ln a$ Relative amplitude change computed down seismic traces is offered in the Seismic Attribute Generation software as an amplitude attribute" (Halliburton-Landmark, 2011). .	2011).
spectral decomposition	"Spectral decomposition refers to any method that produces a continuous time-frequency analysis of a seismic trace"(Castagna	It detects changing in the thickness and the edges of channel.

	and Sun 2006).	
RMS amplitude	"Rms amplitudes are calculated as the square root of the average of the squares of the amplitudes found within an analysis window. The RMS amplitudes are sensitive to sandstone-bearing depositional systems tracts within the reservoir-bearing succession and help define the spatial distribution of genetically related depositional successions" (Michale V. Deangelo and Lesli J. Wood, 2001)..	It could be used to detect unconformities, channel, lithology, and hydrocarbon accumulations.
Envelop amplitude	Envelope amplitude or reflection strength is defined as the root square of square seismic trace	Maximum value of envelope amplitude is interpreted as major changes in the lithology

	plus square quadrature trace (Taner, et al., 1979) .	such as unconformities or presence of gas (Taner, et al., 1979) .
average energy	Average energy is defined as the square of RMS amplitude.	It could be used to detect the area that may has oil or gas. Thus, it is considering as direct hydrocarbon indicators.
Sweetness	"Sweetness s(t) is defined as the trace envelope a(t) divided by the square root of the average frequency fa(t)" $s(t) = \frac{a(t)}{\sqrt{f_a(t)}}$ (Halliburton-Landmark, 2011).	"High sweetness values are those that most likely indicate oil and gas" (Halliburton website). It can be used to detect channel (Hart, 2008).

Table 3-4 Seismic attributes used in this study with description.

Chapter 4- Results

In this section, the results of synthetic seismograms, horizon tracking and surface generation, seismic attributes and well log figures are presented. Three wells were used to match synthetic seismograms with real seismic data (Figures 4-1 to 4-3). Each well has a good quality well log data and all of the data were accepted for synthetic construction. The acoustic impedance of the upper Morrow and lower Morrow formations are low, but the acoustic impedance is high for the Chesteran formation.

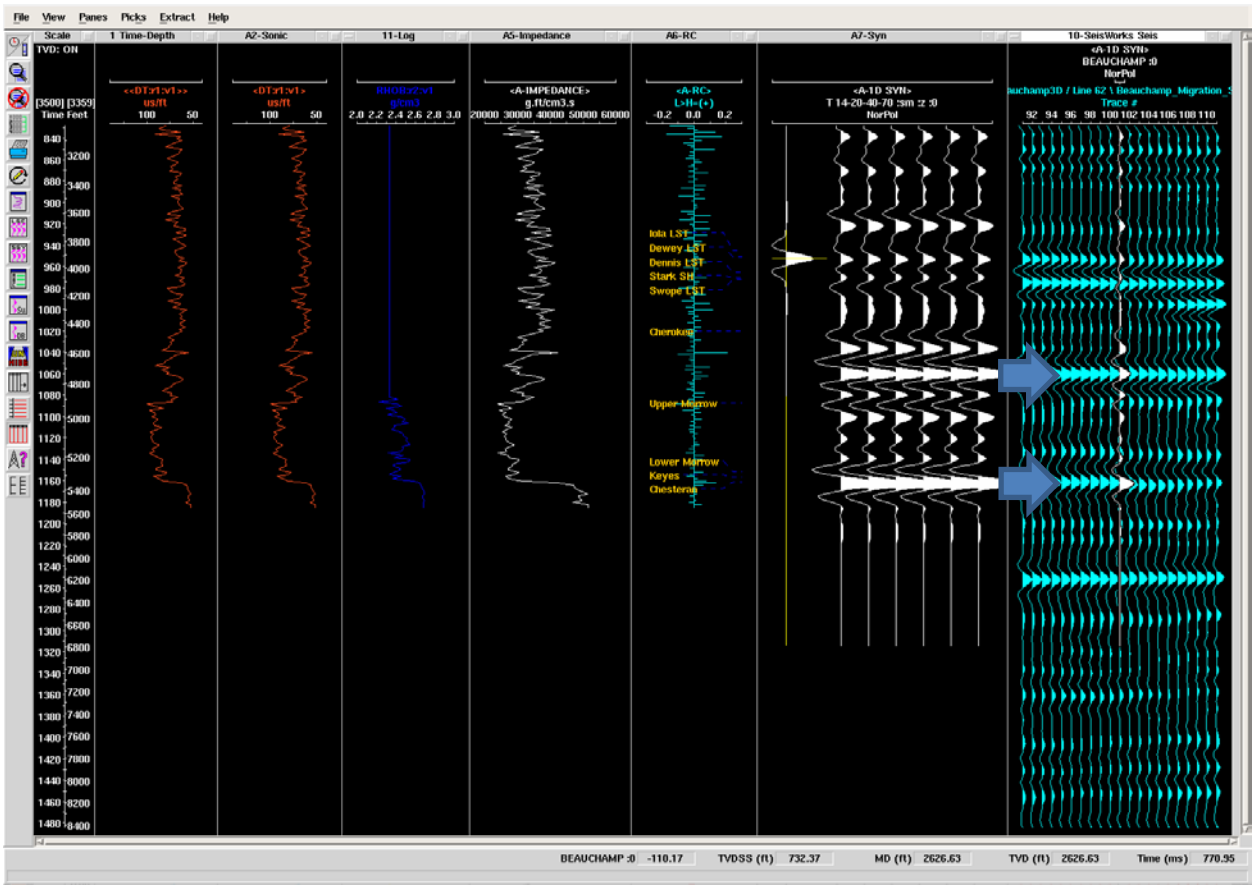

Figure 4-1 Synthetic window for Beauchamp "B" 1 and good match between the synthetic seismogram and seismic data.

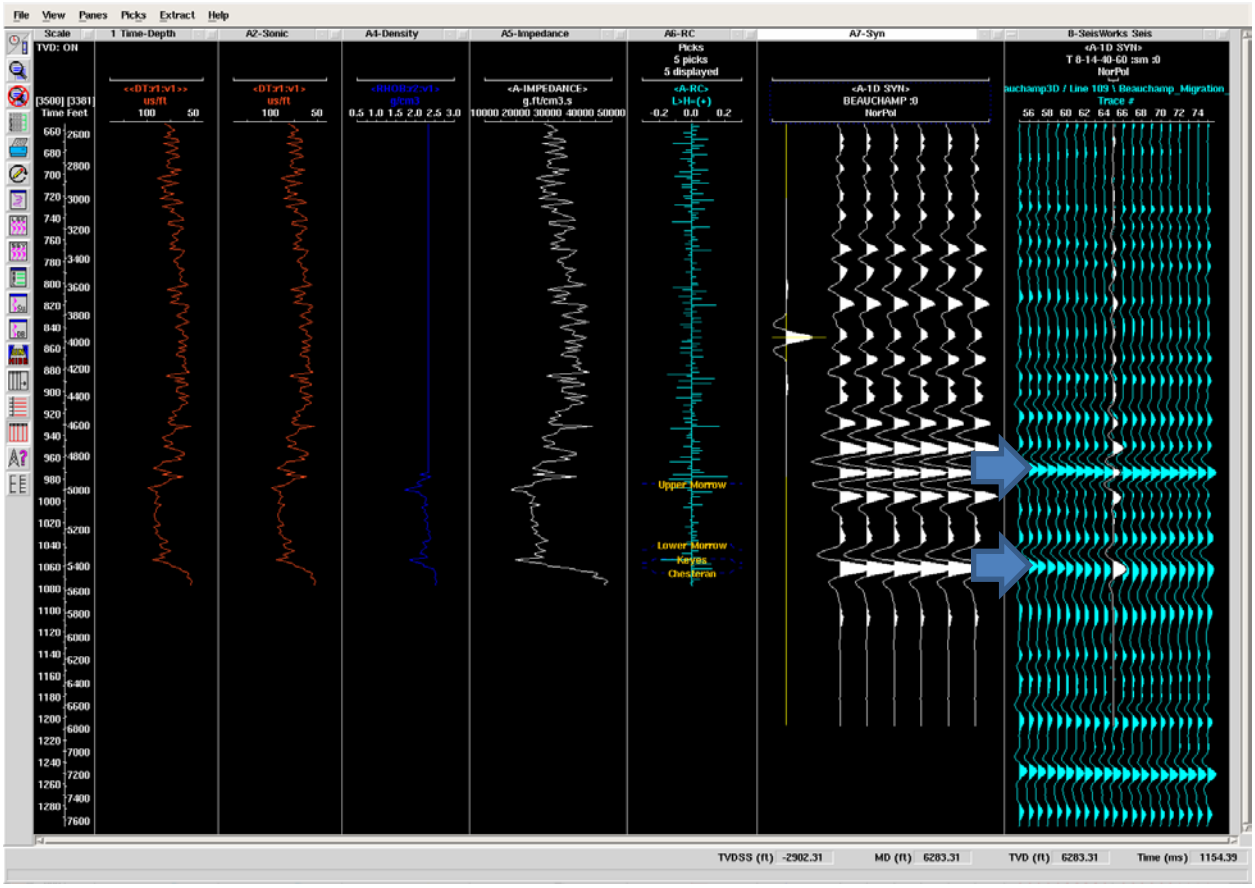

Figure 4-2 Synthetic window for Dicky-robb 1.

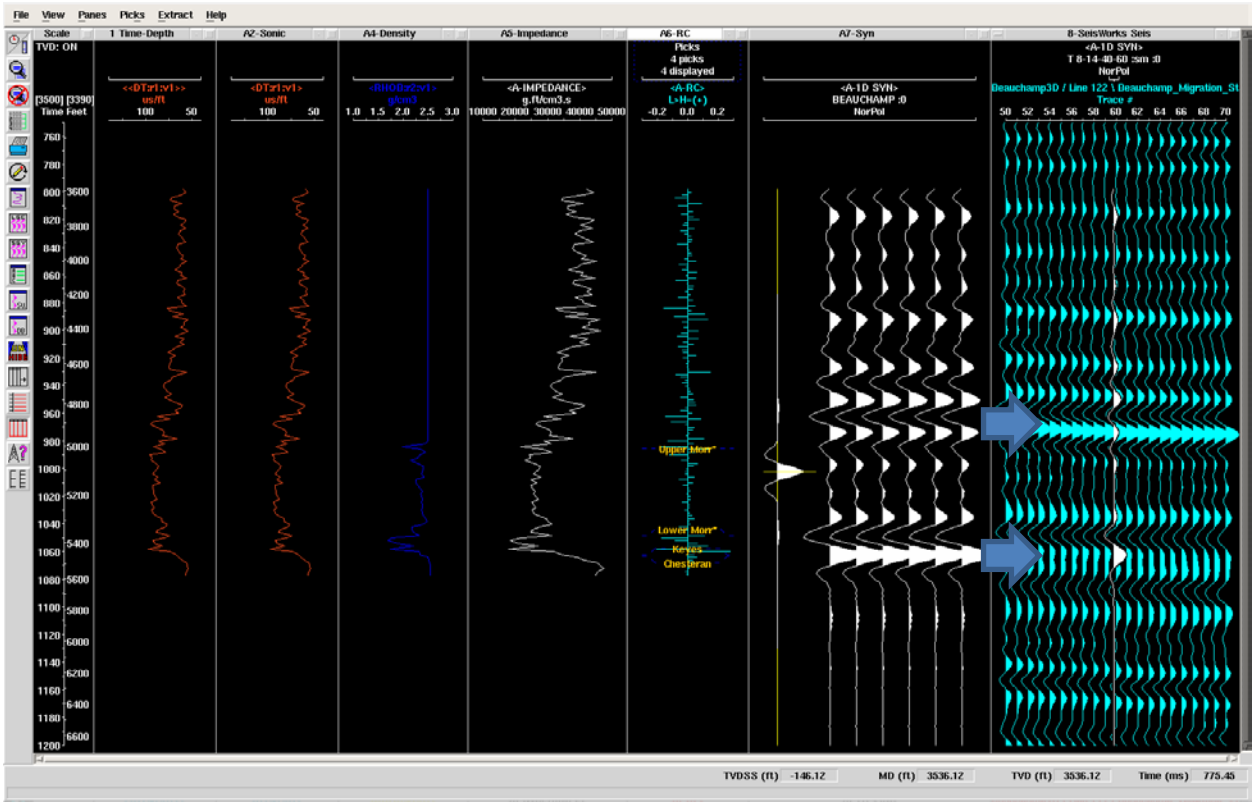

Figure 4-3 Synthetic window for Gwinner 'z' 2

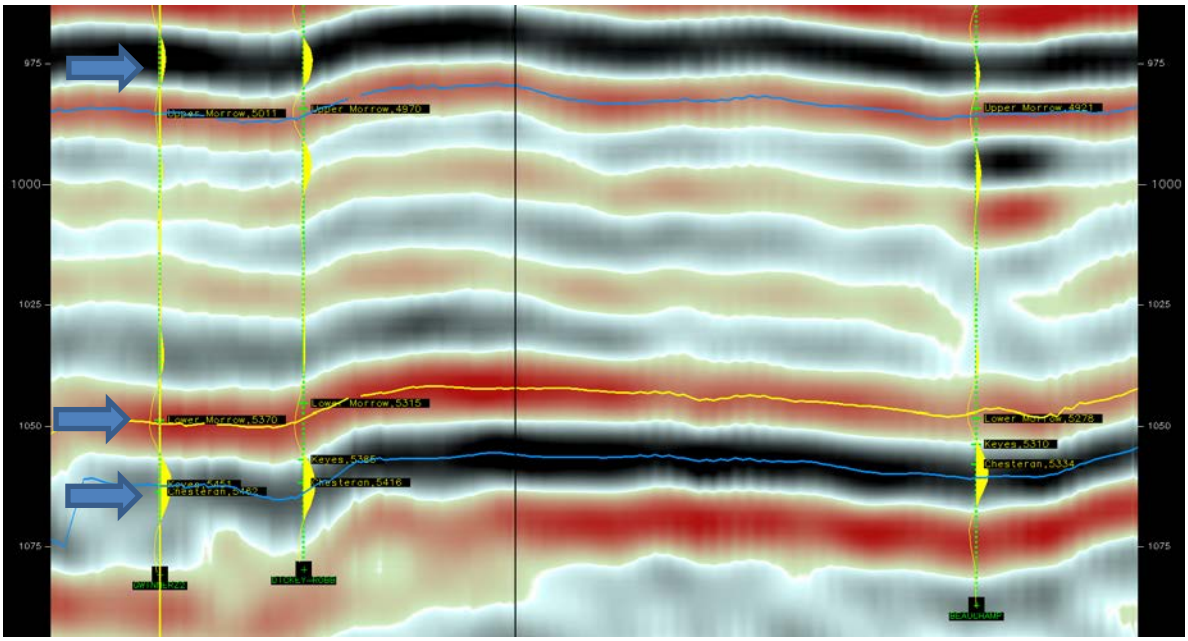

Figure 4-4 Seismic section window illustrating the synthetic seismograms for the three wells matching with seismic data.

The upper Morrow falls in a trough amplitude, which is in red, and the Chesteran falls on the peak amplitude, which is in black (Figure 4-4). Some software such as Seiswork and Petrel has auto-tracking, but auto-tracking wasn't used in this study. Three horizons were chosen for tracking, which were the upper Morrow, the lower Morrow and Chesteran formations. Figure 4-5 shows an example of beginning horizon tracking of upper Morrow formation by using Seiswork software. Figure 4-6 shows how the track progresses through an amplitude. Figure 4-7 shows the completion of a tracked horizon (upper Morrow) along one inline.

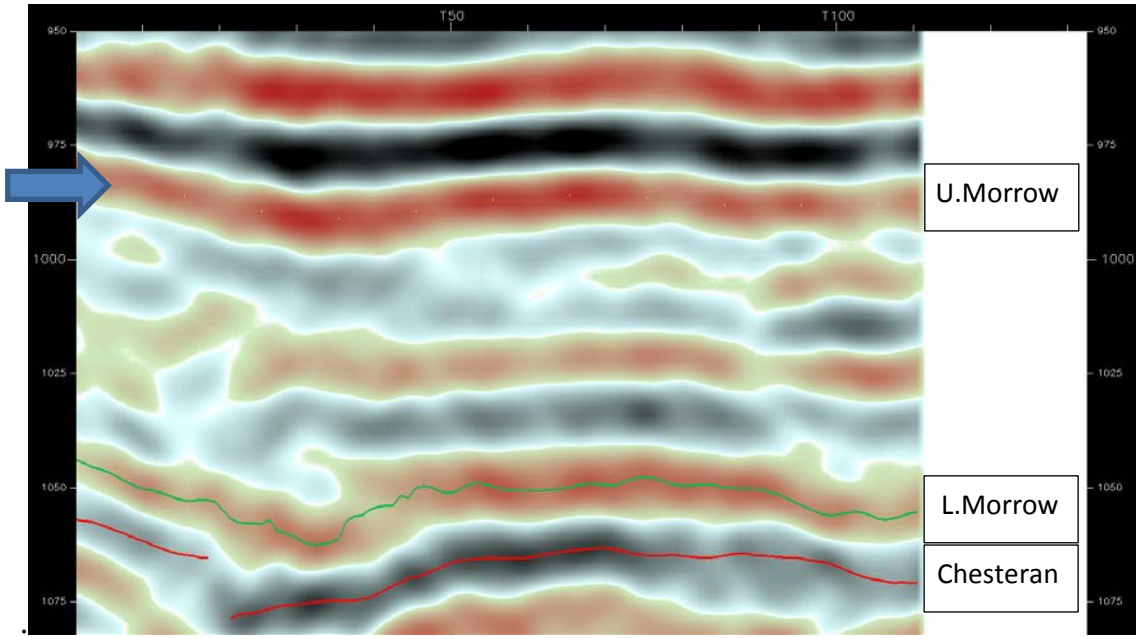

Figure 4-5 Window showing the beginning of tracking the upper Morrow horizon.

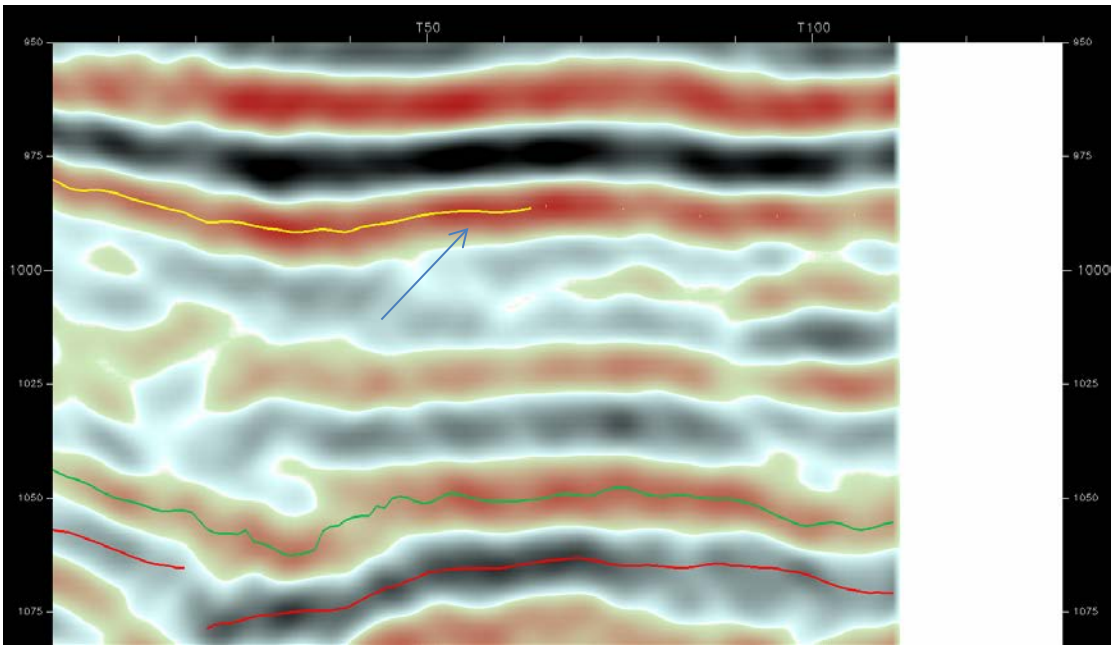

Figure 4-6 Window showing the picking of upper Morrow horizon.

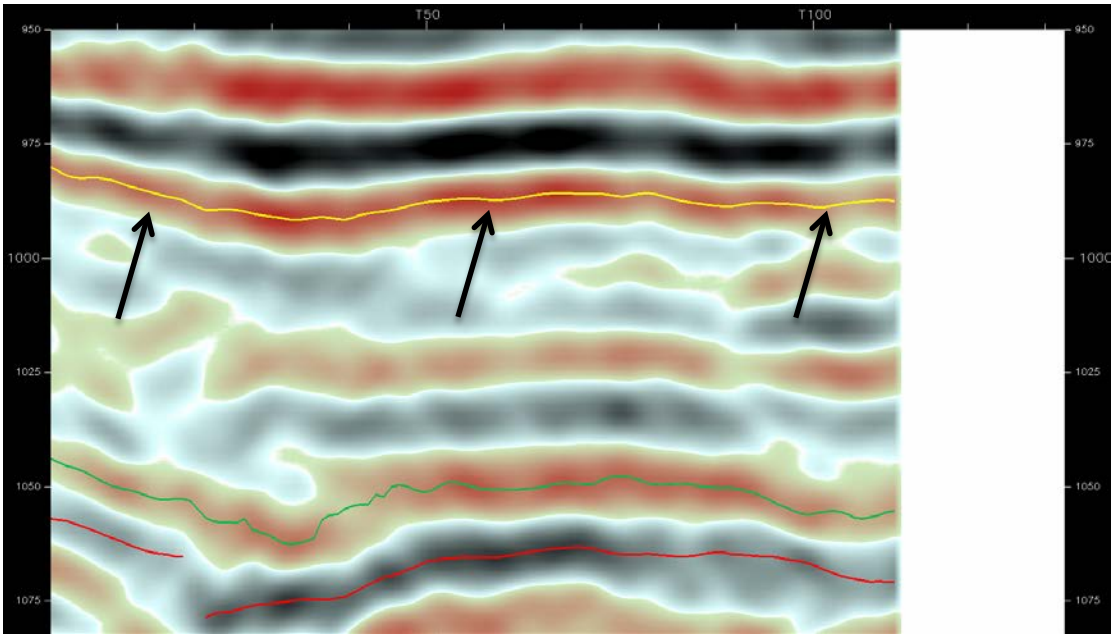

Figure 4-7 Window showing completed picking of upper Morrow horizon in one inline.

Figures 4-8 and 4-9 show how the tracking for each horizon is accounted for on each cross line over the entire seismic cube. It is important to quality check the horizon tracking to insure that the same horizon is picked across the seismic dataset.

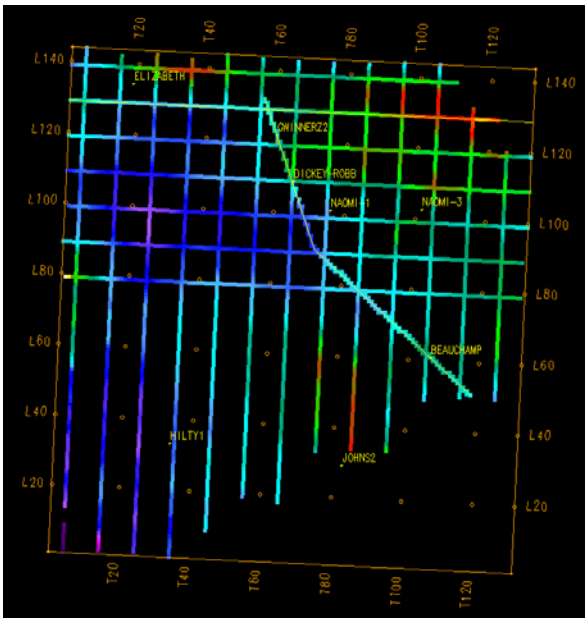

Figure 4-8 Map view showing inlines and Xlines on upper Morrow formation during horizon picking.

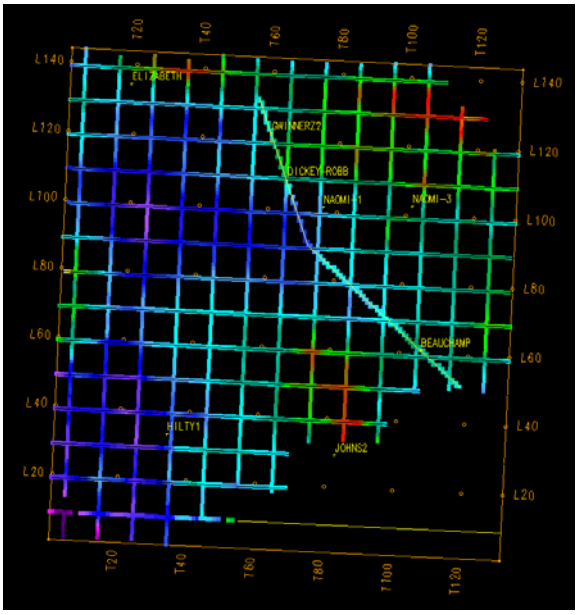

Figure 4-9 Map view of upper Morrow horizon with 10 increment between inline and Xlines.

Three time structure slices were created (Figures 4-10 to 4-13), which shows the time structure of upper Morrow, lower Morrow and Chesteran formations. Figure 4-14 shows a time slice at the top of Incised Valley-fill at 996 ms within upper Morrow formation.

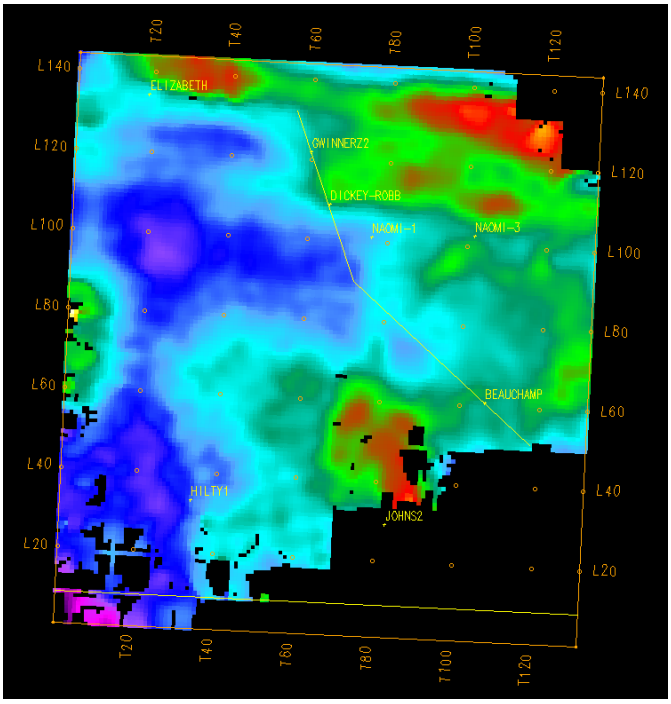

Figure 4-10 Map view of upper Morrow horizon time structure.

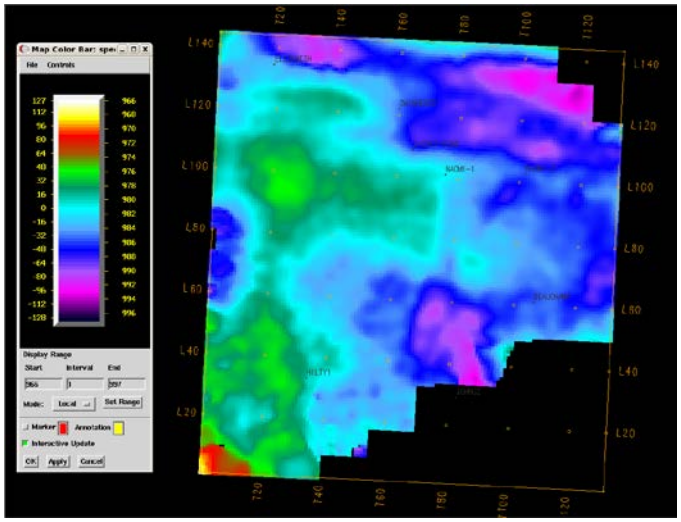

Figure 4-11 Map showing the time structure horizon of upper Morrow formation and s final step of tracking.

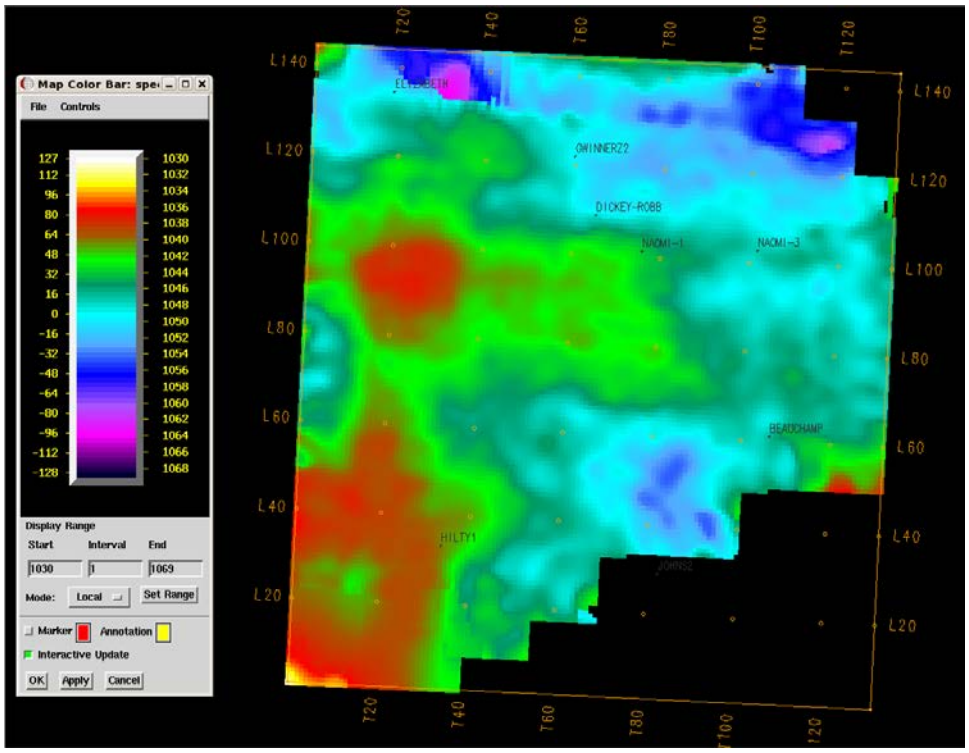

Figure 4-12 Map showing the time structure horizon of lower Morrow formation.

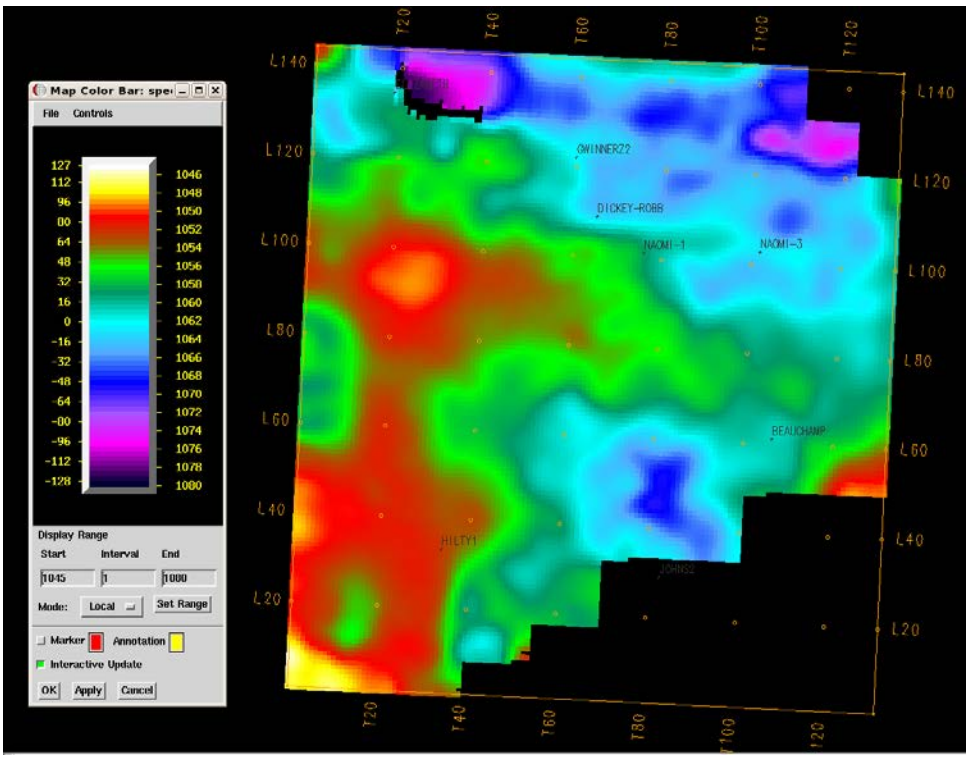

Figure 4-13 Map showing the time structure horizon of Chesteran limestone top.

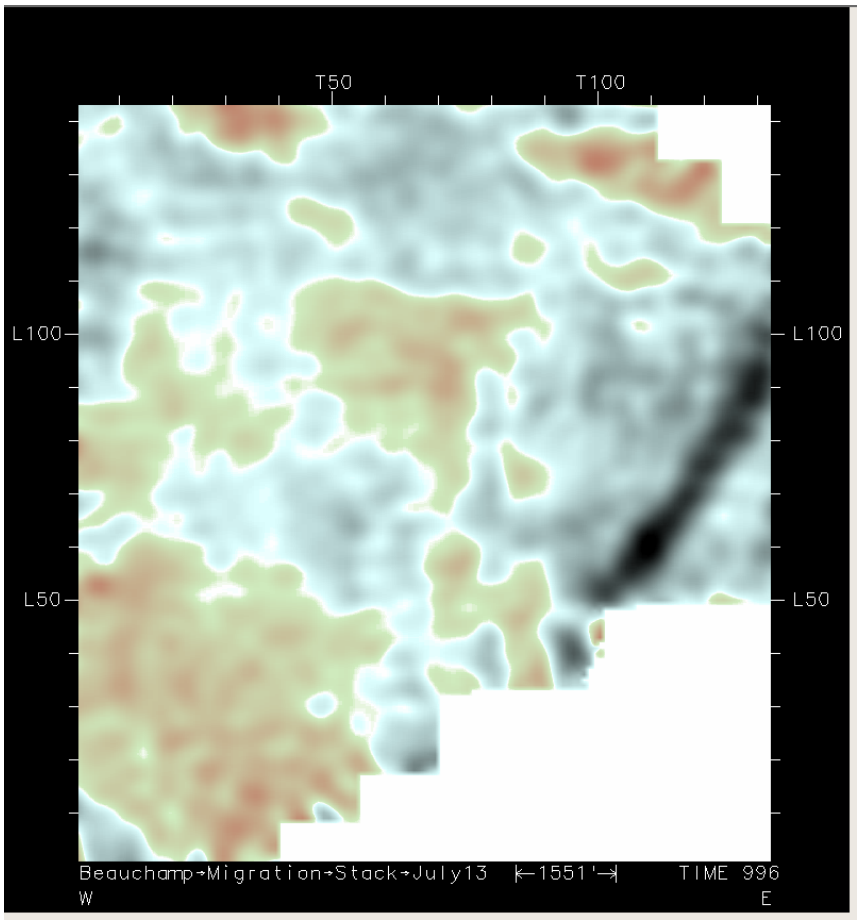

Figure 4-14 Map showing time slice at 996 milliseconds, which hit the top surface of incised valley-fill

Chapter 5 -Discussion

A distinct lineament can be seen in Figure 4-14, along the eastern edge of the map. This is at a time slice that corresponds to the upper Morrow formation. In accordance with the most modern interpretation of Morrow sand deposition in incised valleys as described in a previous chapter, it is possible that the lineament is an incised valley-fill. This will be confirmed by using multiple seismic attributes.

RMS amplitude, average energy, envelope amplitude (reflection strength) and sweetness attributes were used to detect incised valley-fill sand in this study area and to determine if there is the presence of hydrocarbon. On the other hand, coherency, most negative curvature, most positive curvature, discontinuity along dip and amplitude change along X or Y attributes were used to detect incised valley-fill sand and determine its edges and directions. The spectral decomposition attribute was used to determine the thickness of the incised valley-fill sand in the study area. The upper Morrow formation top interval in the seismic section falls on 984 millisecond and the valley-fill sand top falls on 994 millisecond.

The results for RMS amplitude and average energy attributes were almost the same. The upper Morrow horizon, which the target zone (valley-fill sand) falls in is sand. The window interval of RMS amplitude was from the upper Morrow horizon to 35 milliseconds below it, and average energy was 10 milliseconds above the upper Morrow formation and 20 milliseconds below. The RMS amplitude attribute map shows a high anomaly on the incised valley-fill sand (Figure 5-1). The trend of the valley-fill is from southwest to northeast, and shows four areas on the valley-fill sand that have very higher amplitude (bright spots) than the area around it. Bright spots are interpreted as indicating the presence of hydrocarbons, or possibly changes in the lithology in the study area. It may indicate changing lithology from shale to sand because the deposition of Morrow formation was exposed to transgression and regression which deposited sequences of shale and sandstone in the incised valley-fill. The bright spots may be oil accumulations because there is well (Johns 2 – 12), that is located out of the seismic survey boundary, produces oil from a valley-fill sandstone. The Beauchamp 'B' 1 well falls on the extreme edge of the valley-fill sand, and it is dry well. In this situation, the valley-fill acts as a stratigraphic trap, which explains why some wells are located very close to the producing oil wells. The quick lateral change in lithology laterally, losing the good sand, happens as you move

off of the valley-fill. Figure 5-1 is a RMS amplitude map showing four areas that have bright spots in the incised valley-fill sandstone. Figure 5-2 is a RMS amplitude map on the study area.

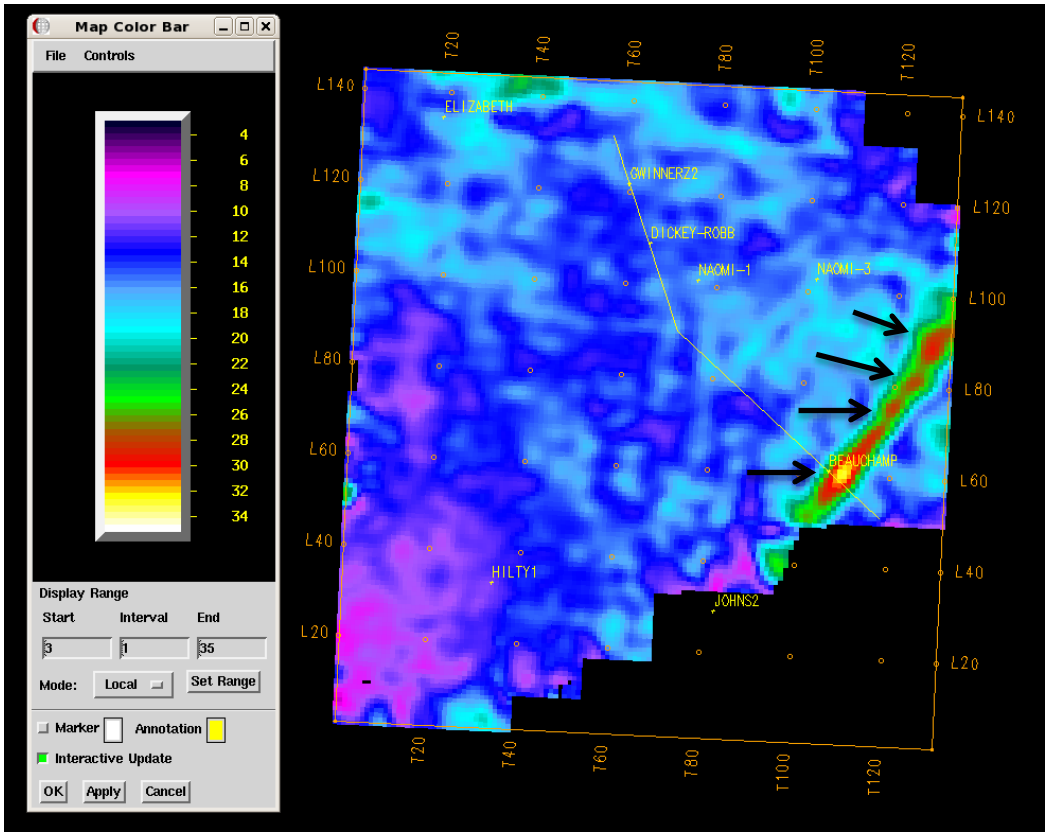

Figure 5-1 RMS amplitude map showing four areas that have bright spots in the incised valley-fill sandstone.

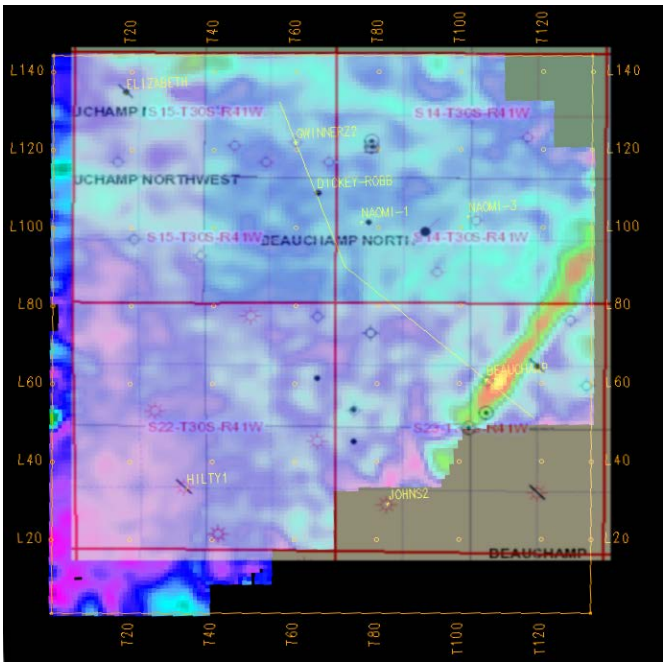

Figure 5-2 RMS amplitude map on the study area.

The average energy also shows the extent of valley-fill sand, with two large areas of high amplitude on the map, and two small areas of high amplitude in the middle of incised valley-fill sand, as seen in Figure 5-3. High energy may be interpreted as contrasting in lithology between shale and sandstone of valley-fill deposits, or are as containing hydrocarbon.

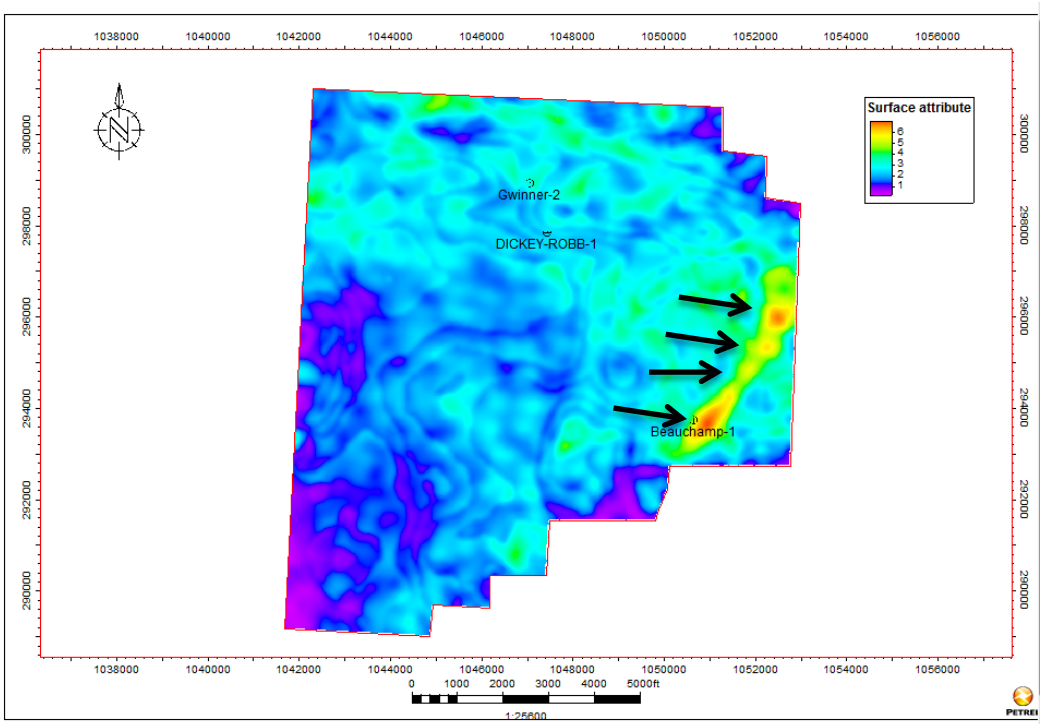

Figure 5-3 Average energy map shows the high position areas which may indicate presence of hydrocarbon or lithologis changes.

The envelope amplitude (reflection strength) slice is at 1000 milliseconds, and displays the extension of all valley-fill sand in the study area. It also shows four areas that have high amplitude, but average energy and RMS amplitude showed the four areas more clearly than envelope amplitude. The high amplitude in envelope map is interpreted as changing of the lithology, although it may indicate hydrocarbon accumulation. It has a vertical window which showed the valley-fill sand very clearly changing laterally. Figure 5-4 shows the envelope amplitude map and Figure 5-5 shows Envelop Amplitude section.

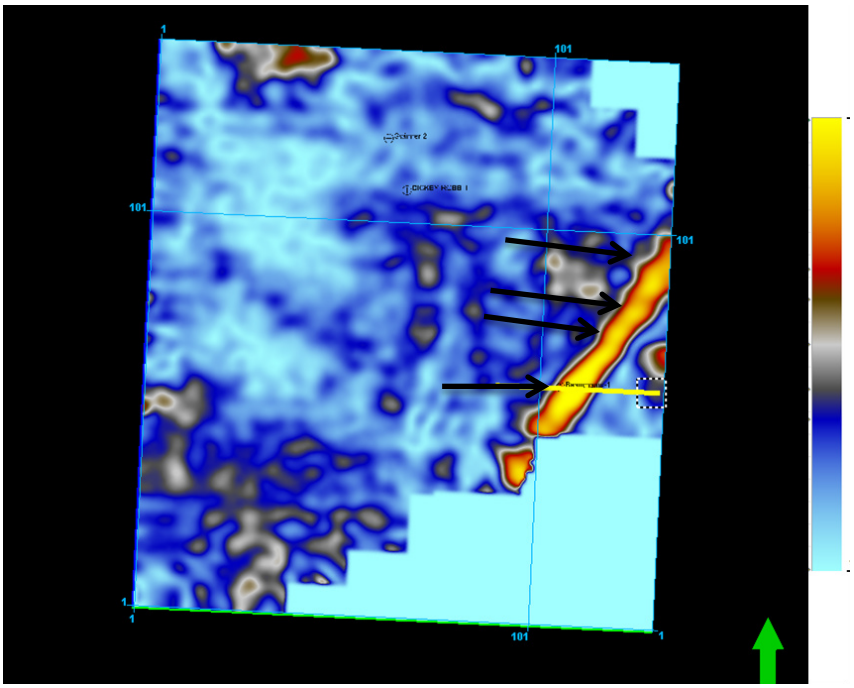

Figure 5-4 Envelop amplitude map showing the extension of incised valley-fill sandstone from north east to south west, and showing the four areas of high amplitude.

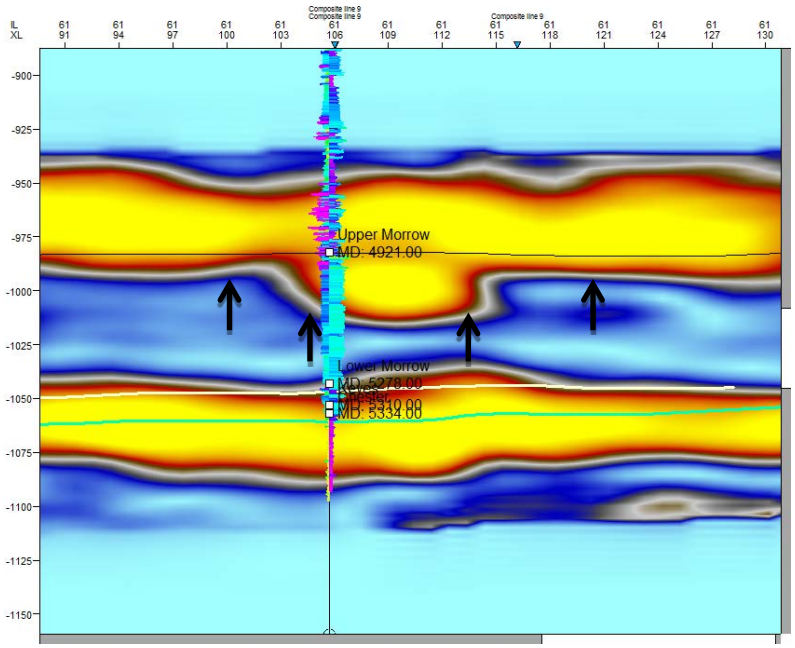

Figure 5-5 Envelop amplitude section showing the lateral anomaly change laterally because of incised valley-fill sandstone.

The sweetness attribute detected the valley-fill sand in the area extremely well. In this study, sweetness detected the edge of the valley-fill sand very clearly but it didn't distinguish the high sweetness contrast between the shale and sandstone within the valley-fill sand, as seen in Figure 5-6. There may not be as large a contrast in acoustic impedance between shale and sand.

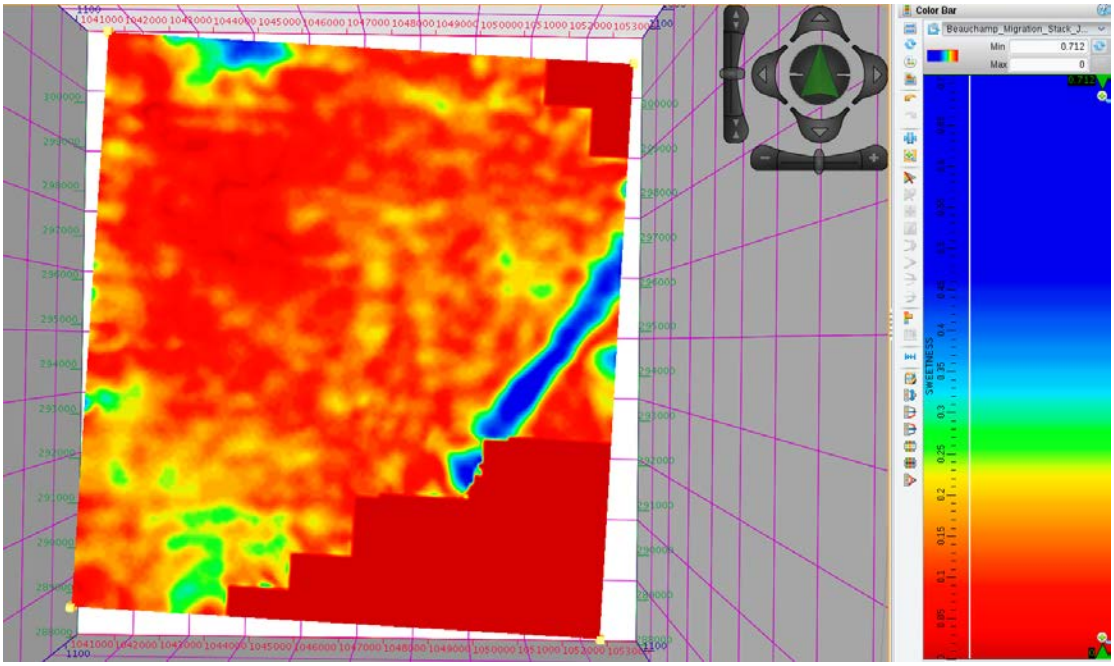

Figure 5-6 Sweetness attribute map showing the extension of incised valley-fill sandstone.

Coherency (discontinuity) and discontinuity along dip attributes maps also display the valley=fill sand in the study area. The valley-fill sand is shown in discontinuity along dip clearer than coherency attribute. The trend of the valley-fill sand from southwest to northeast is the same in all data with RMS amplitude, sweetness, average energy and envelope amplitude. Coherency attribute and discontinuity along dip also show the edge and the width of incised valley-fill sand as shown in Figure 5-7.

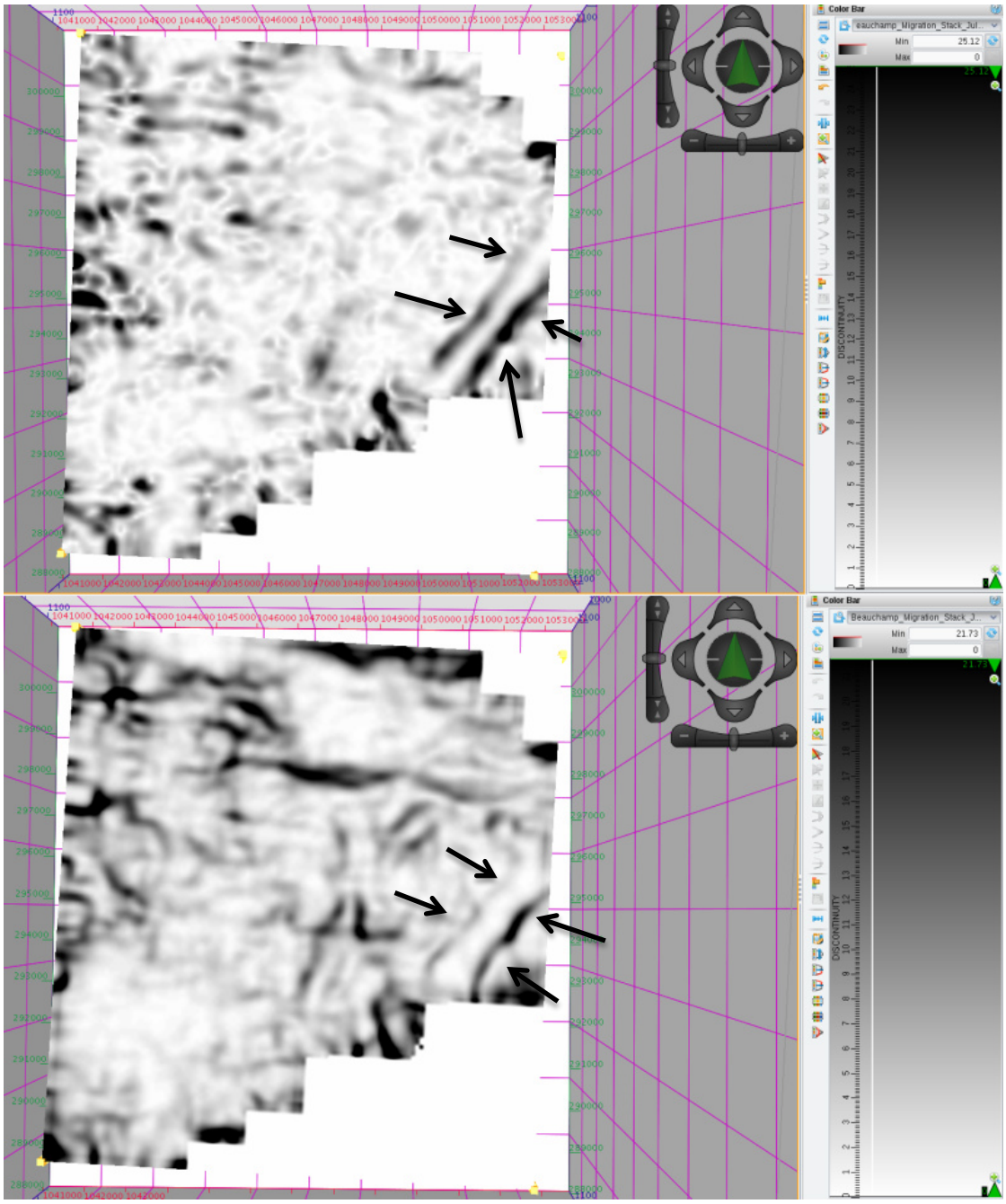

Figure 5-7 Two maps showing the edges of incised valley-fill sandstone. Discontinuity along dip is above the Coherency. Discontinuity along dip exhibits the edges with continuity clearer than Coherency.

As for most positive and negative curvature, positive curvature shows valley-fill sand which may indicate highs in structure, and less compaction over the valley-fill axis. It may also indicate the valley-filled with sand, as seen in figure 5-8. On the other hand, negative curvature in figure 5-9 shows the edge of valley-fill and its center may show shale deposition, based on Chopra and Marfurt, 2012.

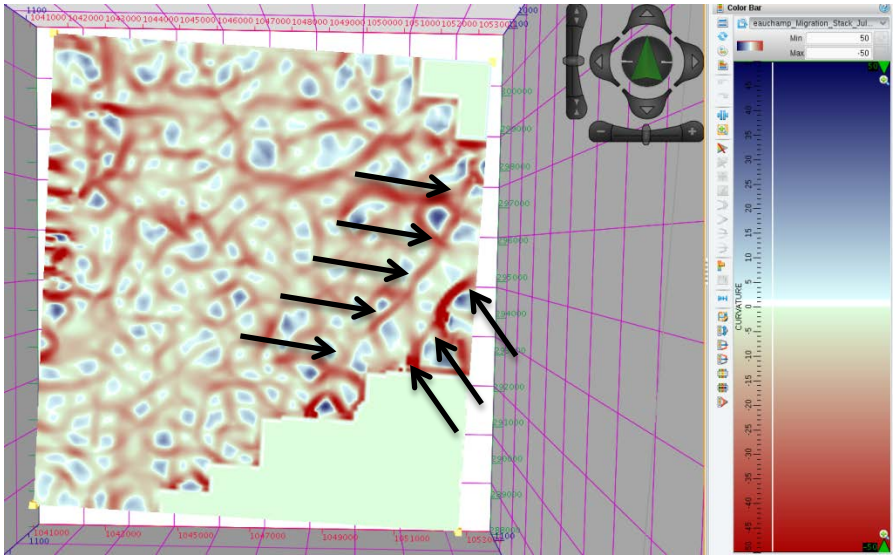

Figure 5-8 Most negative curvature showing edges of valley-fill sand, this may show deposition with shale in center.

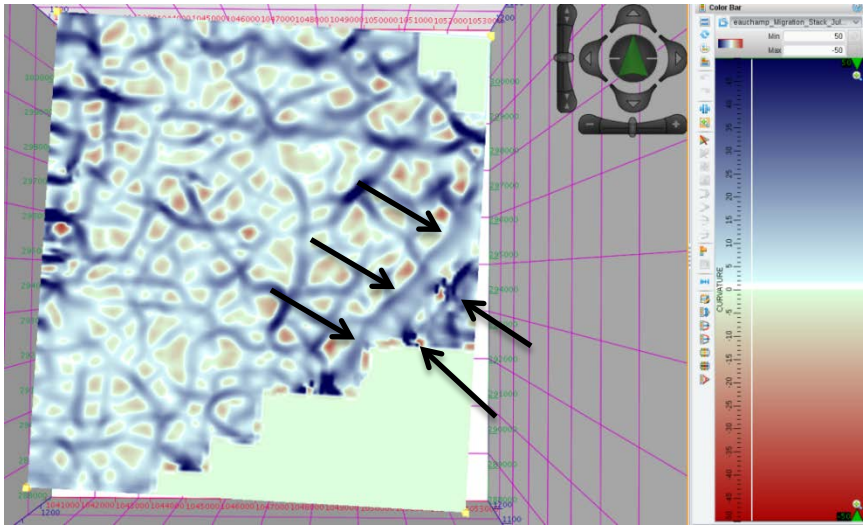

Figure 5-9 Most positive curvature shows center of incised valley-fill sandstone, this may indicate deposition sandstone in center of valley.

Spectral decomposition, using a window interval from 995 to 1020 milliseconds, and was covered the whole valley-fill sand. Frequencies start from 10 to 70 Hz on that window interval. From 10 to 20 Hz, they display the bottom of the valley-fill sand which is thin in the middle and wide in the south and north areas, as seen in figure 5-10. From 30 to 60 Hz, the valley-fill sand become bigger than in lower frequencies and the edges of it become wider than in lower frequencies, as seen in figure 5-11. The valley-fill sand begins to disappear in the spectral decomposition map at 70 Hz, as seen in figure 5-12. Therefore, the frequencies between 10 to 20 Hz suggest the bottom of the valley-fill sand and the frequencies between 40 and 60 suggest the edges of the valley-fill sand.

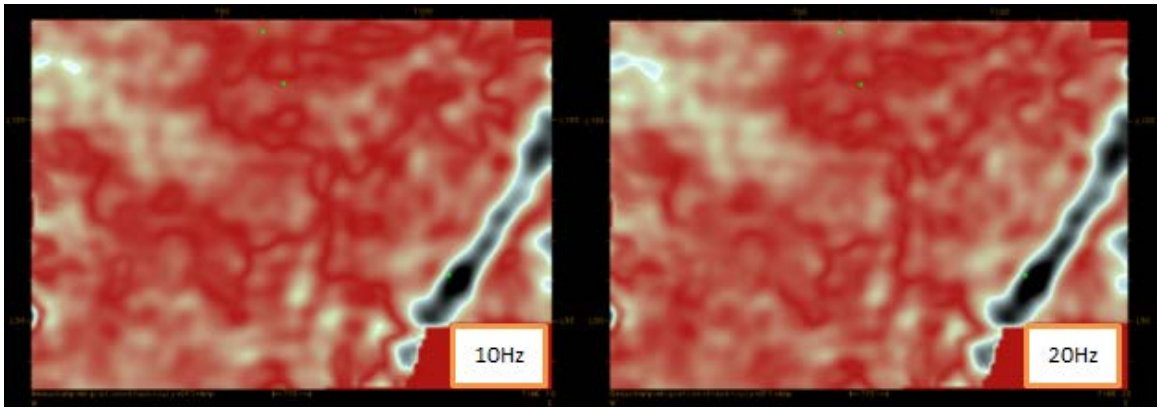

Figure 5-10 Spectral Decomposition defines the thickness of bottom valley-fill sandstone with frequencies from 10 Hz to 20 Hz. Zero Hertz in the left and 10 Hz on the right.

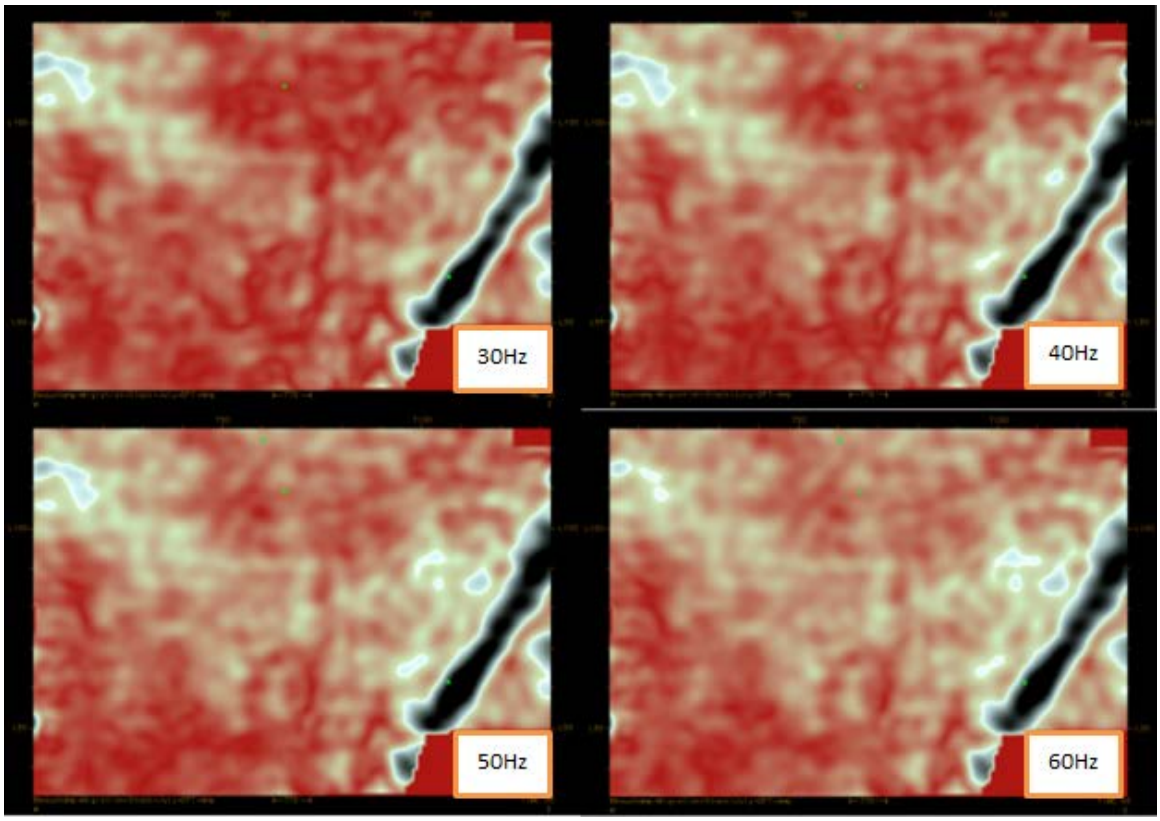

Figure 5-11 Spectral Decomposition showing the thickness of the whole incised valley-fill sandstone from 30 Hz to 60 Hz and the variation in thickness from area to another.

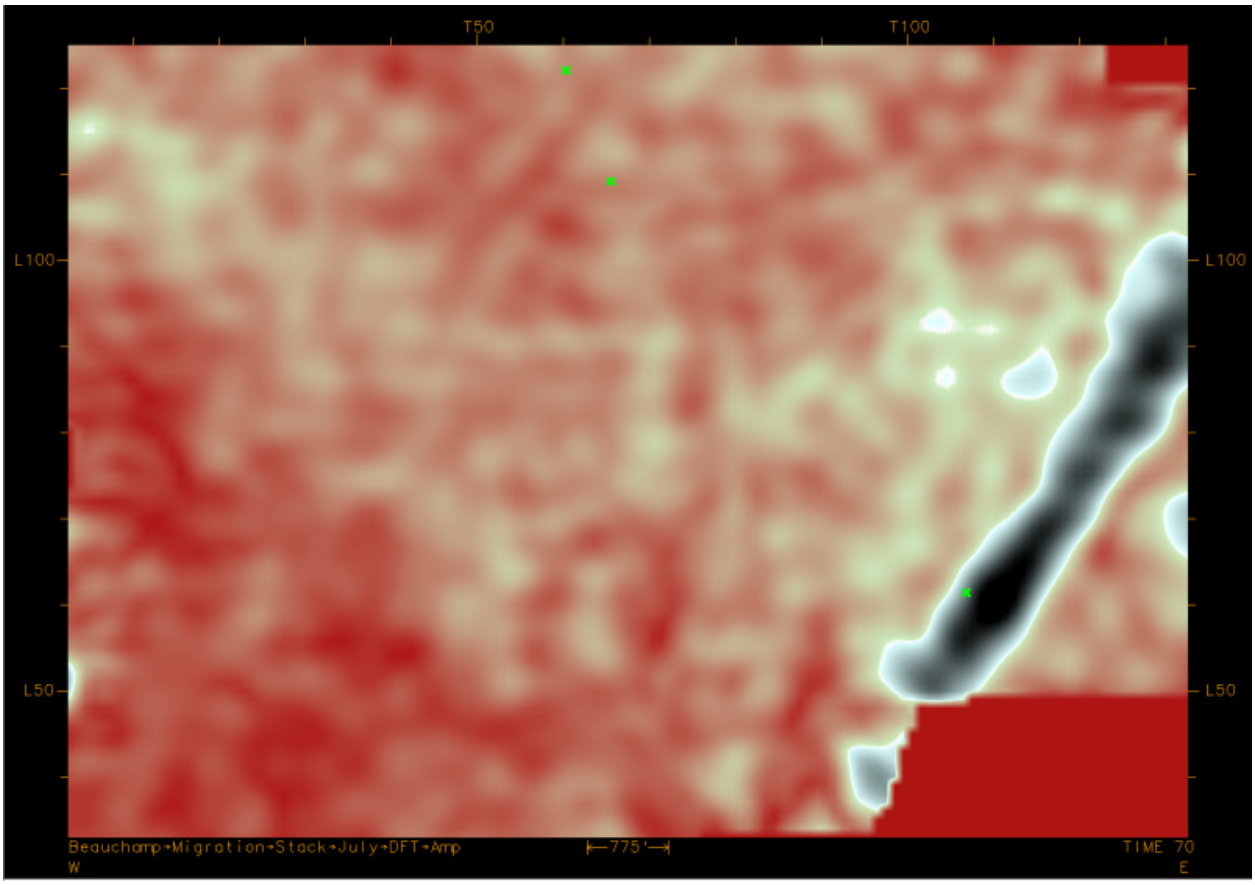

Figure 5-12 Spectral Decomposition showing the edges of the incised valley-fill sandstone in 70 Hz and the variation in thickness.

As for relative amplitude change with X and Y, they were created at 1008 ms. They show the direction and the width of valley-fill sandstone. Relative amplitude change with X shows the pattern change in horizon map with x direction, as seen in figure 5-13. Relative amplitude change with Y shows the pattern change in horizon map with Y direction, as seen in figure 5-14.

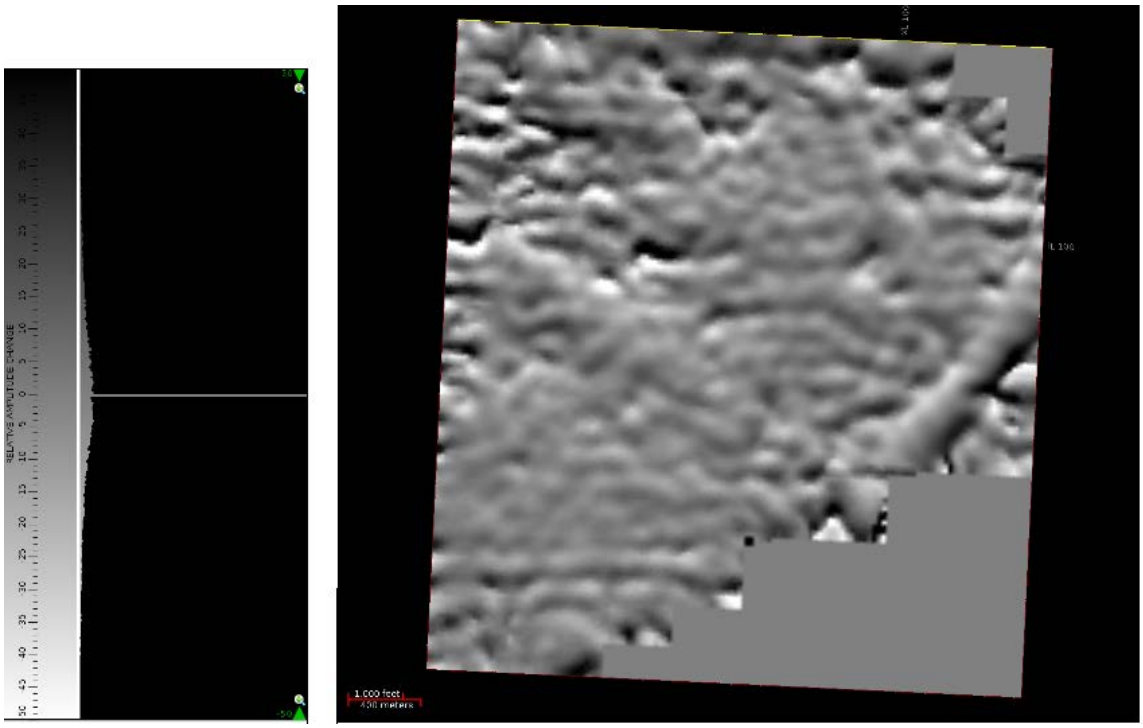

Figure 5-13 Relative amplitude change with X showing the valley-fill in study area.

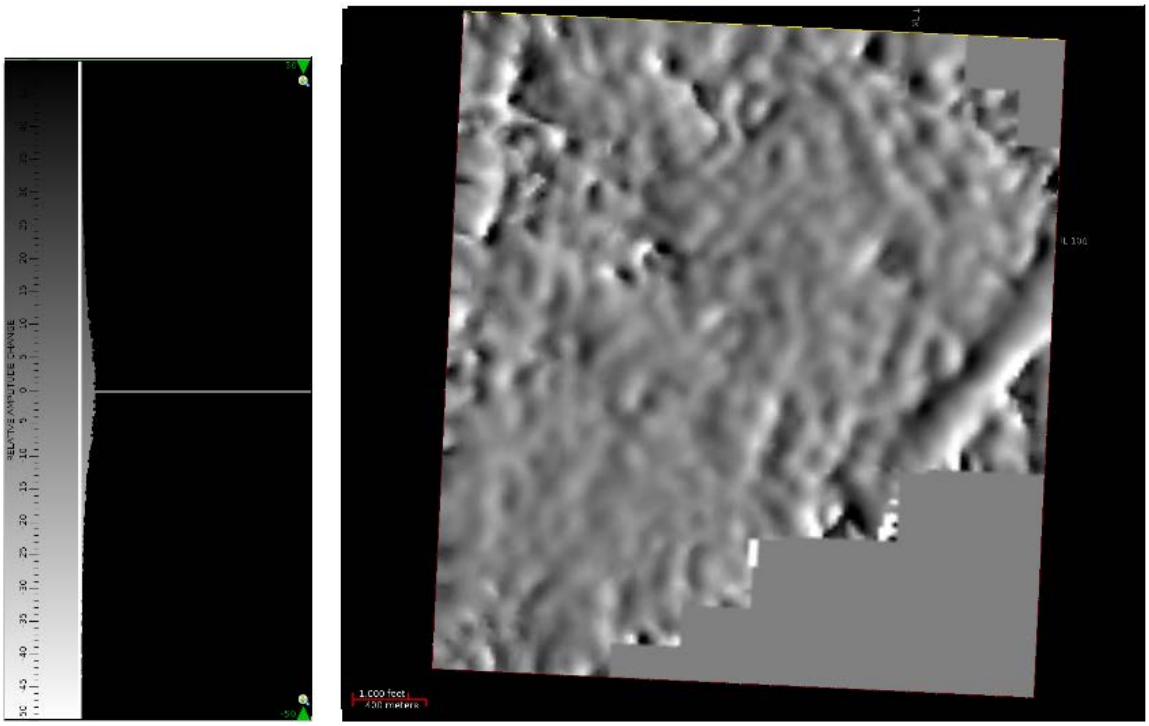

Figure 5-14 Relative amplitude change with Y showing the valley-fill sand in study area.

To cross check the interpretation of a valley-fill sandstone using seismic attributes, a gamma ray cross section using well logs was created. The purpose of using well log correlation is to confirm that there is incised valley-fill sandstone in the area, and also to detect if there is any well that is producing oil in near the valley-fill sand. Gamma ray log and Spontaneous Potential Log were used because these well logs have features that can detect and define if there is sandstone or shale sequences in a well. High gamma ray indicates shale and low gamma ray indicates sandstone.

Eight wells were used in this study because the direction of valley-fill sand tends toward them. One of the wells (Beauchamp 'B' 1) falls on the survey boundary. A gamma ray cross section was made from six wells which begins with Johns 2-12 in the north east and ends with Beauchamp "B" 1 in the south west as seen in Figure 5-15. This Gamma ray cross section correlates Gamma Ray of six wells to define the sequences of the incised valley-fill sandstone. Figures 4-30 to 4-32 show gamma ray and Sp logs of six wells.

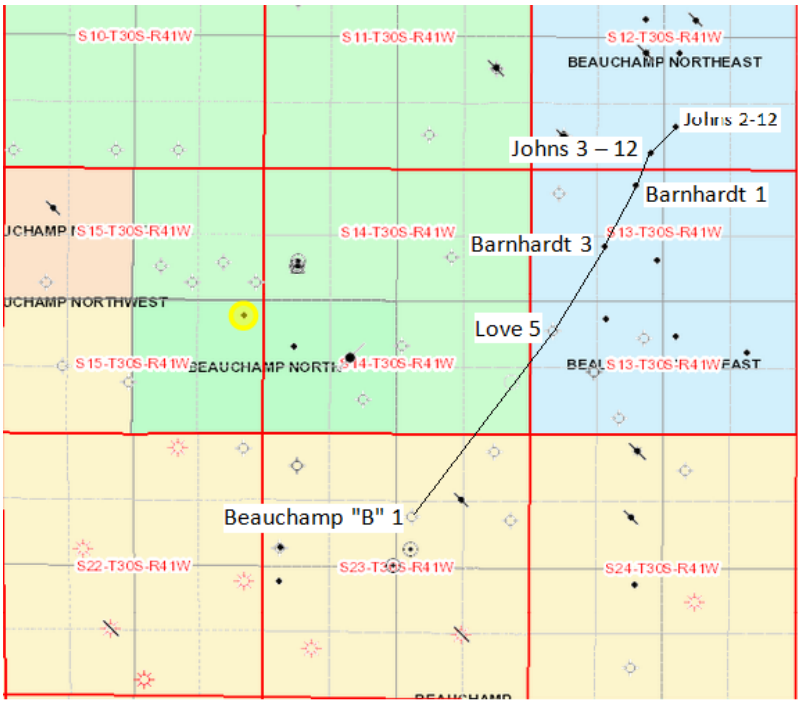

Figure 5-15 Map showing the line of gamma ray cross section with well names[8].

---

[8] **Modified from (Kansas Geological Survey).**

The result of this gamma ray cross section in Figure 5-16 illustrates that there are sequences of valley-fill sand which are reported as sandstone A, B, C and D. Some of wells show all of 4 units of sandstone, while some of the wells don't. This gamma ray cross section also shows that sandstones A and B are the thickest sandstone in the upper Morrow. Structurally, there is decreasing in elevation of these sequences from Johns 2-12 to Branhardt 3, and elevation of these sequences rising from Love to Beauchamp 'B' 1, possible due to a fault. The sandstone A and B doesn't appear very developed in Beauchamp B1 because it falls on the edge of the valley, which would not be expected to have a big thickness of sandstone. Therefore, in the areas that are falling on the middle of valley, sand has a larger thickness of sandstone then the area that is falling on the edge of valley-fill sand. This confirms the interpretation as a valley-fill sandstone.

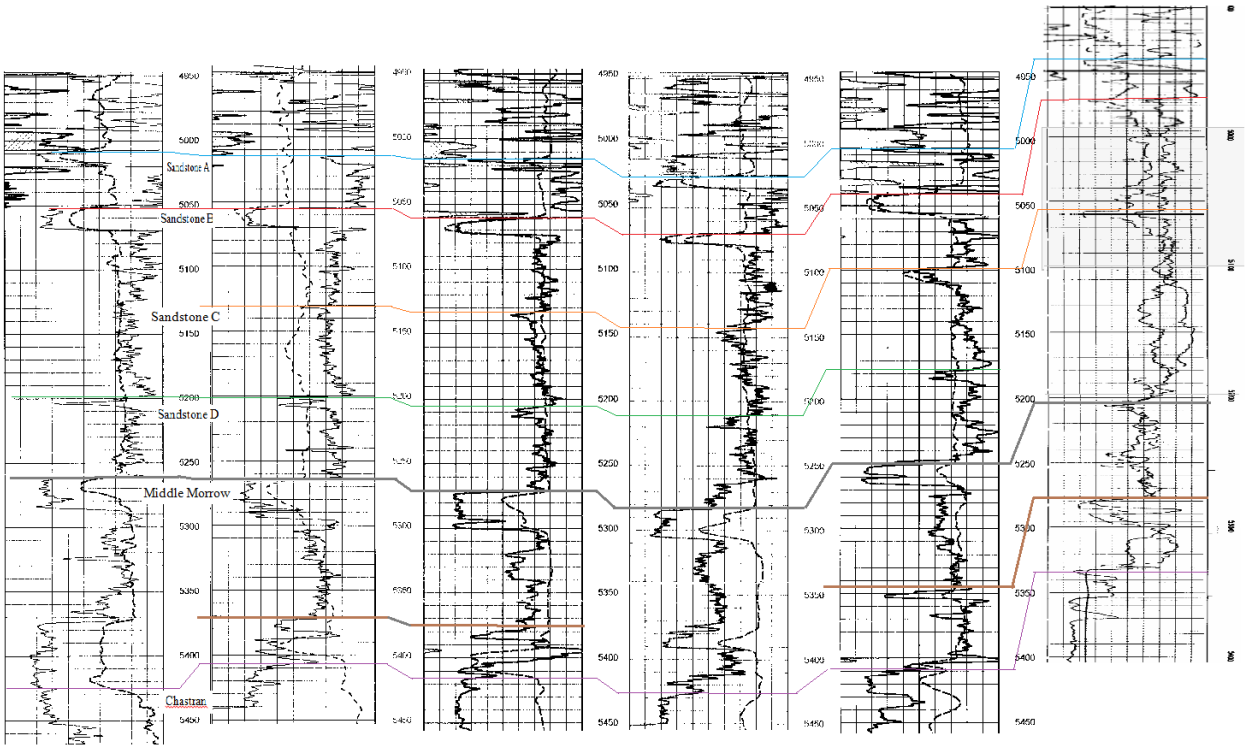

Figure 5-16 Gamma ray cross section showing the correlation between six well from Johns 2-12 (left) to Beauchamp "B" 1.

Chapter 6 – Conclusions and Recommendation

In this study, several seismic attributes such as coherence, spectral decomposition, most positive curvature, most negative curvature , sweetness, discontinuity along dip, average energy, relative amplitude change in X and Y, RMS amplitude and envelop amplitude were used to detect and define valley-fill sand in a 3D seismic survey in Stanton County, Kansas. These attributes may indicate a changing lithology from sand to shale across the valley-fill, and may also indicate the presence of hydrocarbons. RMS amplitude, average energy and envelope amplitude show the incised valley-fill sand, and RMS and average energy also show four areas of high amplitude within the valley. Again, they may indicate changing in lithologies and may also indicate the presence of hydrocarbons. The sweetness attribute detects the valley-fill, but it doesn't show variations between shale and sandstone. Coherency, discontinuity along dip and relative amplitude change with X and Y detect the valley-fill sandstone and are best at determining its width and direction. Spectral decomposition detects the valley-fill sandstone, and also shows the variation in thickness and width of valley-fill. The most negative curvature shows the edges of the valley-fill sandstone best. The most positive curvature shows a structural high in the center of the valley, which may indicate it as filled with sandstone. A gamma ray cross section using well log data shows sequences of incised valley-fill sandstone and variations in their depths from Johns 2-12 to Beauchamp "B" 1. Johns 2-12 well is producing oil from sandstone A and the lower Morrow formation, therefore, the incised valley-fill sandstone may produce oil or gas within the study area because the sequences of incised valley-fill in Beauchamp 'B' 1 are structurally higher in than the other wells.

It is recommended that a test well will be drilled within the outline of the valley-fill, at the areas of highest amplitude.

References Cited

Al-Shaieb, Z., Puckette, J., & Abdalla, A. (1995). Influence of sea-level fluctuation on reservoir quality of the upper Morrowan sandstones, northwestern shelf of the Anadarko Basin, in N. J. Hyne, ed. Sequence stratigraphy of the midcontinent: Tulsa Geological Society Special Publication, no.4, p. 429- 268.

Castagna, J. P., & Sun, S. (2006). Comparison of spectral decomposition methods: First Break, volume 24 75-79.

Chopra, S., & Marfurt, K. J. (2007), Seismic attributes for prospect identification and reservoir characterization.

Chopra, S., & Marfurt, K. J. (2012). Seismic attribute expression of differential compaction.

Deangelo, M. V., & Wood, L. J. (2001). 3-D seismic detection of undrilled prospective areas in a mature province, South Marsh Island, Gulf of Mexico.

Forgotson, J., Miller, A., & David, M. (1966). Influence of regional tectonics and local structure on deposition of Morrow Formation in western Anadarko Basin: AAPG Bulletin, v. 50, p. 518-532.

Gerken, L. D. (1992) Morrowan sandstones in south-central Texas County, Oklahoma: Oklahoma State University unpublished M.S. thesis, 140 p.

Hart, B. S. (2008). Channel detection in 3-D seismic data using sweetness.

Halliburton-Landmark. (2011). Discontinuty along dip. Retrieved from http://esd.halliburton.com/support/LSM/DSD/DSD/5000/5000_8/Help/mergedProjects/attributes/discontinuity_along_dip.htm

Halliburton-Landmark. (2011). Most negative curvature. Retrieved from http://esd.halliburton.com/support/LSM/DSD/DSD/5000/5000_8/Help/mergedProjects/attributes/most_neg_curvature.htm

Halliburton-Landmark. (2011). Relative amplitude change in x or y. Retrieved from http://esd.halliburton.com/support/LSM/DSD/DSD/5000/5000_8/Help/mergedProjects/attributes/xy_rel_amp_change.htm

Halliburton-Landmark. (2011). Sweetness. Retrieved from http://esd.halliburton.com/support/LSM/DSD/DSD/5000/5000_8/Help/mergedProjects/attributes/sweetness.htm

Kansas academy science, Map of Kansas Counties, Retrieved from http://www.kansasacademyscience.org/files/sympos96/price/county.htm.

Kansas Geological Survey.. (2013). Stanton County. Retrieved from http://maps.kgs.ku.edu/oilgas/index.cfm?extenttype=well&extentvalue=1006155029.

Kristinik, L., & Blakeny, B. (1990). Sedimentology of the upper Morrow Formation in eastern Colorado and western Kansas in Sonnenberg et al. eds. Morrow sandstones of southeast Colorado and adjacent areas: Denver, The Rocky Mountain Association of Geologists p. 37-50.

Moore, G. E. (1979). "Pennsylvanian paleogeography of the southern Mid-Continent.": 2-12

NeuraLog. (2013). Automated well log digitizing software. Retrieved from http://www.neuralog.com/pages/NeuraLog.html

Newell, K. D., Watney, W. L., Cheng, S. W. L., & Brownrigg, R. L. (1987) Stratigraphic and spatial distribution of oil and gas production in Kansas: Kansas Geological Survey, Subsurface Geology Series 9, 86 p.,

Northern Arizona University. (2010). Paleogeography and Geologic Evolution of North America , Retrieved from http://www2.nau.edu/rcb7/nam.html

Potonie, H. (1911). Die Tropen-Sumpfflachmoor-Natur der Moore des produktiven carbone, in Kgl. Preuss. Geol. Landesanstalt, Berlin, Jahrb. 1909: v. 30, pt. 1, p. 389-443.

Puckette, J., Abdalla, A., Rice, A., & Al-Shaieb, Z. (1996). The upper Morrow reservoirs: complex fluvio-deltaic depositional systems, in Johnson, K., ed., Deltaic reservoirs in the southern midcontinent, 1993 symposium, Oklahoma Geological Society Circular, no. 98, p. 47-84.

Rascoe, B. Jr. (1978). Late Paleozoic structural evolution of the Las Animas arch: in Pruit, J. D., & P.E. Coffin (eds.), Energy Resources of the Denver basin, RMAG Guidebook, p. 113-127.

Rascoe, B., Jr., and F. Adler, (1983). Permo-Carboniferous hydrocarbon accumulations, Mid-Continent, USA: AAPG Bulletin, v. 67, p. 979-1001

Schlumberger Oilfield Glossary. (2013). attribute. Retrieved from http://www.glossary.oilfield.slb.com/en/Terms.aspx?LookIn=term name&filter=attribute.

Schopf, J. (1975). Pennsylvanian climate in the United States, in Mckee ed, Paleotectonic investigations of the Pennsylvanian System in the United States, part II. USGS professional paper 853, p 23-31.

Sonnenberg, S. (1985) Tectonic and sedimentation model for Morrow sandstone deposition, Sorrento field area, Denver Basin: Mtn. Geol. v. 22, p. 180-191.

Sonnenberg, S., Shannon, L., Kathleen, R., & Drehle, W. V. (1990). Regional structure and stratigraphy of the Morrowan Series, southeast Colorado and adjacent areas, in Sonnenberg, S., et al. eds. Morrow sandstones of southeast Colorado and adjacent areas: Denver, The Rocky Mountain Association of Geologists p. 1-8

Stephen, M. T. (1994). Geological Aspects of Hazardous Waste Management.

Swanson, D. C. (1979). Deltaic deposits in the Pennsylvanian upper Morrow formation of the Anadarko Basin, in Pennsylvanian sandstones of the Mid-continent: TGS Pub. No. 1, p. 115-168.

Taner, M. T., Koehler, F., & Sheriff, R. E. (1979). Complex seismic trace analysis.

Wheeler, D., Scott, A., Coringrato, V., & Devine, P. (1990). Strtigraphy and depositional history of the Morrow Formation, southeast Colorado and southwest Kansas in Sonnenberg, S., et al. eds. Morrow sandstones of southeast Colorado and adjacent areas: Denver, The Rocky Mountain Association of Geologists p. 9-35.

White, D. (1913). Physiographic conditions attending the formation of coal, in White, David, and Thiessen, Reinhardt, The origin of coal, with a chapter on the formation of peat, by C. A. Davis: U.S. Bur. Mines Bull. 38, p. 52-84.

White, D. (1932). The carbonaceous sediments, in Twenhofel, W. H., & others, Treatise on sedimentation [2d ed., rev.]: Baltimore, Williams & Wilkins, p. 351-430.